# Intracellular pH regulation in $H^+$-ATPase-rich ionocytes in zebrafish larvae using *in vivo* ratiometric imaging

Hong Meng Yew

Thesis submitted to the

Faculty of Graduate and Postdoctoral Studies

University of Ottawa

In partial fulfillment of the requirements for the

Master of Science in Biology Degree in the

Ottawa-Carleton Institute of Biology

September 30, 2016

**Acknowledgements**

First of all, I would like to thank my supervisor, Dr. Steve Perry for his constant guidance and support throughout the course of the project. Thank you especially for all your advice and help, without which the project would not have been possible to be completed successfully. I would also like to thank my committee members Drs Kathleen Gilmour, Marc Ekker and Michael Jonz for their valuable input and suggestions made throughout my committee meetings.

Secondly, I would like to thank all the members of the Perry and Gilmour labs, past and present, for their constant support and making my life as a graduate student an enjoyable one. Special thanks to RK and VT for contributing invaluable help and advice, and also KL for working with me on the experiments, and for the interesting discussions which contributed much to the development of the technique and the data analysis.

Thirdly, I would like to thank Peter Andrew Ochalski for working with me on figuring out the technical aspects which made our experiments possible, and also Vishal Saxena for taking care of the fish I worked with all the time.

I would also like to thank my family for their understanding and unwavering support, for me to pursue a higher level of education and a career in Biology.

Last but not least, I would also like to thank Dr. Steve Perry again and the University of Ottawa for the financial support throughout the course of my Master's program, and also to the Natural Sciences and Engineering Research Council (NSERC) of Canada Discovery and Research Tools grants to Dr. Steve Perry for the funding of this project.

**Table of Contents**

**List of Figures**

**List of abbreviations**

$^{0}$C --- Celsius

μg --- Microgram

μm --- Micrometer

μL --- Microliter

ANOVA --- Analysis of variance

ATP --- Adenosine triphosphate

BCECF --- 2',7'-bis-(2'-carboxyethyl)-5',6'-carboxyfluorescein

BSA --- Bovine serum albumin

Cas --- CRISPR associated protein

CCAC --- Canadian Council of Animal Care

CCCP --- Carbonyl cyanide m-chlorophenyl hydrazine

cDNA --- Complementary deoxyribonucleic acid

ConA --- Concanavalin A

CRISPR --- Clustered regularly interspaced short palindromic repeats

Dpf --- Days post fertilization

EMCCD --- Electron multiplied charge coupled device

ENaC --- Epithelial $Na^{+}$ channel

FRET --- Förster resonance energy transfer

FW --- Freshwater

HA --- $H^{+}$-ATPase

HR --- $H^{+}$-ATPase rich

KS – $K^{+}$-secreting

L --- Liter

LED --- Light-emitting diode

Min --- Minute

mL --- Milliliter

mM --- Millimolar

MO --- Morpholino

NAR --- $Na^+/K^+$-ATPase rich

NCC --- $Na^+/Cl^-$ co-transporting

NHE --- $Na^+/H^+$ exchanger

nm --- Nanometer

NMR --- Nuclear magnetic resonance

PBS – Phosphate buffered saline

PCR --- Polymerase chain reaction

PFA --- Paraformaldehyde

PFBI --- Potassium-binding benzofuran isophalate

pHi --- Intracellular pH

ROI --- Region of interest

RT-PCR --- Reverse transcriptase polymerase chain reaction

SFBI --- Sodium-binding benzofuran isophalate

SIET --- Scanning ion-selective electrode technique

SLC --- Solute carrier

SNARF --- Seminaphthorhodaflour

SW --- Seawater

TBS --- Tris buffered saline

V --- Volt

**Abstract**

The $H^+$-ATPase rich (HR) cells of zebrafish larvae are a sub-type of ion-transporting cell located on the yolk sac epithelium that are responsible for $Na^+$ uptake and $H^+$ extrusion. Current models of HR cell ion transport mechanisms in zebrafish larvae are well established, but little is known about the involvement of the various ion transport pathways in regulating intracellular acid-base status. In the present study, a ratiometric imaging technique using the pH indicator dye BCECF was developed to monitor intracellular pH (pHi) continuously in larval zebrafish HR cells *in vivo*. Initial validation experiments demonstrated that HR cells subjected to respiratory acidosis (1% $CO_2$) or metabolic alkalosis (20 mM $NH_4Cl$) exhibited changes in BCECF 513/438 emission ratios which were consistent with the expected effects of these treatments on pHi. Subsequent experiments focussed on the involvement of the two principal apical membrane acid excretory pathways, the $Na^+/H^+$ exchanger (isoform NHE3b; *zslc9a3.2*) and the $H^+$-ATPase (*atpv1aa*) in pHi regulation. Additionally, the role of HR cell carbonic anhydrase ("CA2-like a") was investigated because of its presumed role in providing $H^+$ for $Na^+/H^+$ exchange and $H^+$-ATPase. To do so, relative HR cell pHi changes were monitored during acid-base challenges in shams and in fish experiencing morpholino gene knockdown of either NHE3b, $H^+$-ATPase or "CA2-like a". The temporal pattern and extent of intracellular acidification during exposure of fish to 1% $CO_2$ and the extent of post-$CO_2$ alkalization were altered markedly in fish experiencing knockdown of "CA2-like a", NHE3b or $H^+$-ATPase. Although there were slight differences among the three knockdown experiments, the typical response was a greater degree of intracellular acidification during $CO_2$ exposure and a reduced capacity to restore pHi to baseline levels post-hypercapnia. Knockdown of "CA2-like a", although presumed to limit $H^+$ availability to NHE3b and $H^+$-ATPase, yielded qualitatively similar results to knockdown of

either single $H^+$ excretory pathway. The metabolic alkalosis and subsequent acidification associated with $NH_4Cl$ exposure and its washout were largely unaffected by gene knockdown. Overall, the results suggest markedly different mechanisms of intracellular acid-base regulation in zebrafish HR cells depending on the nature of the acid-base disturbance.

**Résumé**

Les cellules riches en $H^+$-ATPase (RH) dse larves de poisson-zèbre sont un sous-type de cellules de transport d'ions situées sur l'épithélium du sac vitellin et qui sont responsables de l'absorption du $Na^+$ et l'expulsion des ions $H^+$. Les modèles actuels de mécanismes de transport d'ions dans les cellules RH des larves de poisson-zèbre sont bien établies, mais on connaît mal l'implication des différentes voies de transport d'ions dans la régulation de l'état acido-basique intracellulaire. Dans la présente étude, une technique d'imagerie ratiométrique a été mise au point pour mesurer le pH intracellulaire (pHi) de façon continue dans les cellules RH de poisson-zèbre larvaires *in vivo*. Des expériences de validation initiales ont montré une capacité des cellules RH à réguler le pHi lorsqu'elles sont soumises à une acidose respiratoire (1% de $CO_2$) ou à une alcalose métabolique (20 mM $NH_4Cl$). Des expériences ultérieures ont porté sur l'implication des deux principales voies excrétrices des acides dans la membrane apicale : l'échangeur $Na^+/H^+$ (isoforme NHE3b; zslc9a3.2) et la $H^+$-ATPase (atpv1aa), dans la régulation du pHi. En outre, le rôle de l'anhydrase carbonique ("CA2-like a") dans la cellule RH a été étudié en raison de son rôle présumé dans la production d'$H^+$ pour l'échangeur $Na^+/H^+$ =et pour la $H^+$-ATPase. Pour ce faire, les changements relatifs de pHi dans la cellule RH ont été suivis au cours d'un défi acide-base chez des poissons subissant une perte de fonction génique à l'aide d'oligonucléotides de type morpholino. Les gènes suivants furent inactivés : NHE3b, $H^+$-ATPase ou "CA2-like a". Le profil temporel et l'amplitude de l'acidification intracellulaire lors de l'exposition des poissons à 1% de $CO_2$ ainsi que l'amplitude de l'alcalinisation post-$CO_2$ ont été modifiées de manière marquée chez les poissons ayant perdu la fonction de"CA2-like a", de NHE3b ou de $H^+$-ATPase. Malgré de légères différences entre les trois expériences de perte de fonction, la réponse

typique était un plus grand degré d'acidification intracellulaire pendant l'exposition au $CO_2$ et une capacité réduite à restaurer le pHi aux niveaux de référence post-hypercapnie. Le perte de fonction de "CA2-lika a", bien que présumée limiter la disponibilité des $H^+$ pour NHE3b et $H^+$ ATPase, a donné des résultats qualitativement similaires à ceux obtenus lors de la perte de fonction de chacune des deux voies excrétrices des $H^+$. L'alcalose métabolique et l'acidification subséquente associées à l'exposition au $NH_4Cl$ (et à son rinçage) n'ont pas été affectées de manière significative par une perte de fonction génique. Dans l'ensemble, les résultats suggèrent des mécanismes de régulation intracellulaire acide-base nettement différents dans les cellules HR de poisson-zèbre en fonction de la nature de la perturbation acido-basique.

## Introduction

Mechanisms of pH regulation

The maintenance of intracellular pH (pHi) is a process of paramount importance across various animal species. The main goal of pHi regulation is to maintain a relatively stable acid/base environment for the various proteins/enzymes to function optimally in the different biological processes taking place inside the cell. The process of pHi regulation takes place in almost all animal-derived cell types, with the exception being non-nucleated erythrocytes (reviewed in Roos and Boron, 1981).

The process of pHi regulation comprises of two distinct components: The capacity of cells to buffer pHi within the cells, and proteins/enzymes involved in acid/base transport which are required to counteract the changes to the pHi. The steady state pHi may be influenced by a variety of factors, such as changes in extracellular pH (Rothe, 1984) and induced changes by extracellular factors such as hypercapnia and high external ammonia (Boron and de Weer, 1976). Intracellular buffering of pHi can be achieved through open-system buffers such as the $CO_2/HCO_3^-$ and the $NH_3/NH_4^+$ buffer pairs, which account for the majority of buffering at pHi values close to the resting pHi (reviewed in Roos and Boron, 1981). In cases of acute pHi changes which cannot be counteracted by open-system buffers, pHi regulation can also be conducted through the use of proteins/enzymes involved in acid/base transport. These proteins/enzymes consists of two major groups: Acid extruders that remove acid/introduce base from the cell such as $Na^+/H^+$ exchangers (Murer *et al*., 1976) and $Na^+$-driven $Cl^-/HCO_3^-$ exchangers (Thomas, 1977), and acid loaders that remove base/introduce acid into the cell such as $Cl^-/HCO_3^-$ anion exchangers (Vaughan-Jones, 1979).

The majority of acid/base regulation in vertebrates takes place in specialized cells in the kidneys, where pHi is maintained through a combination of processes such as $HCO_3^-$ reabsorption, ammonia excretion and $H^+$ excretion (reviewed in Malnic, 1988; Yucha, 2004). These processes are essential in counteracting the minute changes that occur in various bodily fluids on a daily basis, and thus are a key mechanism in maintaining pH homeostasis throughout the whole organism.

Osmoregulation in freshwater fish

Freshwater (FW) fish live in an environment with highly different osmotic and ionic properties compared to their body fluids. In contrast to marine fish, FW fish are constantly challenged by the diffusive loss of ions to the hypoionic environment. Thus, FW fish have evolved efficient mechanisms of hyperionic regulation able to match the loss of ions, via the active uptake of ions by specialised epithelial cells (Krogh, 1938).

The exact mechanism whereby ionic homeostasis is maintained in FW fish has been subjected to study and speculation over the past decades, particularly for the abundant ions such as $Na^+$, $Cl^-$ and $Ca^{2+}$ (reviewed in Varsamos et al., 2005). Early studies on goldfish (*Carassius auratus*) suggested the presence of $Na^+/NH_4^+$ and $Cl^-/HCO_3^-$ exchange mechanism (Maetz and Garcia Romeu, 1964). The results of Subsequent studies on goldfish and other teleosts species implicated a $Na^+/H^+$ exchange system for $Na^+$ absorption (Kerstetter *et al*., 1970, Maetz, 1973, Evans *et al*., 1979) thus suggesting a relationship between ionic and acid-base regulation. Further evidence for $Na^+/H^+$ exchange was derived from experiments showing an involvement of carbonic anhydrase (CA) in $Na^+$ uptake (Maetz and Garcia Romeu, 1964, Kerstetter *et al*., 1970,

Payan *et al*., 1975). Clearly, acid-base regulation and $Na^+$ regulation are intricately related in FW fishes.

Currently, there are two major models which have been established, explaining how acid-base regulation is linked to $Na^+$ uptake in FW fishes. In one model, $Na^+/H^+$ exchanger (NHE) is located on the apical surface of epithelial cells, which enables both $Na^+$ uptake and $H^+$ extrusion simultaneously (Wright and Wood, 1985). In a second model, $Na^+$ uptake and $H^+$ extrusion remain linked but function as distinct electrically coupled components, namely an epithelial Na channel (ENaC) or related cation channel and a $H^+$-ATPase (HA) proton pump, respectively (Avella *et al*., 1987, Lin and Randall, 1991).

Discovery of ionocytes in fish

The gill is the major site of ionic uptake in adult FW teleosts. Initially, the presumptive ion-transporting cells were termed "chloride cells" following the discovery of their involvement in active chloride secretion from the blood to the surrounding water in the marine teleost *Fundulus heteroclitus* (Philpott, 1968). Later studies identified the presence of these cells in a variety of teleost species (Iwai, 1969, Roberts *et al*., 1973, Shen and Leatherland, 1978, Foskett and Scheffey, 1982). The chloride cells were demonstrated to be able to secrete $Cl^-$ directly (Karnaky *et al*., 1976), while their involvement in fish ionic regulation was suggested by their close link with $Na^+$ transport (Dharmamba *et al*., 1975, Girard and Payan, 1977, Evans, 1980), the presence of basolateral $Na^+/K^+$-ATPase activity (Karnaky *et al*., 1976, Hootman and Philpott, 1979) and high mitochondrial content (Marshall and Nishioka, 1980, Scheffey *et al*., 1983) .

Interestingly, later studies revealed differences between "chloride cells" of fishes acclimated to FW and marine environments, either in the form of different cellular morphologies

(Peek and Youson, 1979, Girard and Payan, 1980, Hossler *et al*., 1985) or by the presence of neighbouring accessory cells that were found only in fish acclimated to seawater (SW; Pisam *et al*., 1987, 1988). In addition, evidence began to accumulate suggesting the involvement of FW chloride cells in the uptake of other ions such as $Na^+$ and $Ca^{2+}$ (e.g. Perry and Wood, 1985, Urasa and Wendelaar Bonga, 1987). Because of the difference between the morphology and functions of these cells between SW- and FW-acclimated fish, the term "chloride cell" no longer appropriately described these cells in fish in general. Thus, the terms "mitochondrion-rich cell" and "ionocyte" eventually came into use to describe the specialized cells involved in ion regulation in fish in general.

More recent studies on a variety of FW fish model species including fugu (*Takifugu rubripes*), killifish (*Fundulus heteroclitus*), trout (*Oncorhynchus mykiss*), tilapia (*Oreachromis mossambicus*) and zebrafish (*Danio rerio*) (reviewed in Hwang et al., 2011, Dymowska et al., 2012) have shown that different species have developed unique ionocyte sub-types, each responsible for a particular facet of ionic regulation.

Larval zebrafish as an experimental model

During recent years, the zebrafish has been one of the most well studied model organisms on FW fish ion regulation. To date, five distinct subtypes of ionocytes have been identified on the yolk sac epithelium of zebrafish larvae (Guh *et al*., 2015); namely the $H^+$-ATPase rich (HR) cells involved in $H^+$ extrusion and $Na^+$ uptake (Yan *et al*., 2007), the $Na^+/K^+$-ATPase rich (NAR) cells which are involved in transepithelial $Ca^{2+}$ transport (Liao *et al*., 2007), the $Na^+/Cl^-$ co-transporting (NCC) cells involved in both $Na^+$ and $Cl^-$ uptake (Wang *et al*., 2009), the SLC26

cell which functions in $Cl^-$ uptake (Bayaa *et al*., 2009) and the $K^+$-secreting (KS) cells whose function is still not fully known but implied to be related to $K^+$ homeostasis (Abbas *et al*., 2011).

The zebrafish HR cells is arguably the best studied of the different zebrafish ionocyte subtypes, with detailed models explaining the various pathways of $Na^+$ uptake and acid extrusion by the cell, and the roles of the various proteins/enzymes involved (Fig. 1). "CA2-like a", a HR-cell specific paralog of the intracellular carbonic anhydrase 2 found in mammals, is located within the cell and is responsible for the catalysis of the reaction between gaseous $CO_2$ and soluble bicarbonate ions ($HCO_3^-$) and protons ($H^+$) (Lin *et al*., 2008). Rhesus glycoproteins Rhcg1 and Rhbg are localized to the apical and basolateral membranes of the HR cell, respectively, and are involved in ammonia excretion (Nakada *et al*., 2007, Braun *et al*., 2009). The basolateral anion exchanger 1b (AE1b) is responsible for $HCO_3^-/Cl^-$ exchange (Lee *et al*., 2011), while basolateral aquaporin 1 a1 (Aqp1a1) mediates the entry and exit of water to and from the HR cells (Kwong *et al*., 2013).

The HR cell is a prime candidate for investigating the mechanisms of acid-base regulation in zebrafish larvae. The presence of both $H^+$-ATPase and the $Na^+/H^+$ exchanger NHE3b in the HR cells (Yan *et al*., 2007) fits into both proposed models of FW fish acid-base regulation, while the presence of "CA2-like a" in the cytoplasm is thought to provide the $H^+$ to fuel $Na^+/H^+$ exchange and $H^+$ extrusion via the $H^+$-ATPase (Lin *et al*., 2008). Also, the zebrafish HR cell is functionally equivalent to the Type-A intercalated cells, which is a cell type that specializes in $H^+$ secretion and $HCO_3^-$ reabsorption in mammalian kidneys (Kim *et al*., 1999).

Additionally, the zebrafish is a highly versatile model organism with well-established protocols (Westerfield, 1994). For example, there are a variety of molecular biology tools available to be used with zebrafish, including antisense morpholino gene knockdown (Nasevicius

and Ekker, 2000), targeted gene knockout techniques including the recent CRISPR-Cas9 system (Sung *et al*., 2014), and methods for the generation of transgenic lines (Higashijima *et al*., 1997). These tools allow the specific targeting and selective inhibition of proteins/enzymes of interest in the zebrafish HR cell.

Ratiometric imaging

Currently, there is a variety of methods available which can be used to measure pHi in cells. One of the earliest methods is the use of pH-sensitive microelectrodes to directly measure cell pHi while minimizing damage to the cells (Carter *et al*., 1967). Later techniques included the use of high-resolution nuclear magnetic resonance (NMR) techniques to track pHi in real time in cell cultures (Gillies *et al*., 1981), pH-sensitive dyes to visualize the pHi of cells (Grynkiewicz *et al*., 1985). Since the current project hinges on the successful tracking of pHi in live zebrafish larvae in an *in vivo* context, it was decided that the ratiometric pH-sensitive dye technique is the most appropriate for the project's requirements.

Ratiometric ion-selective dyes are able to shift their respective excitation/emission profiles depending on the concentration of the ion of interest in the surrounding solution in which the dye is placed. A key advantage of using ratiometric dyes over conventional fluorescent dyes is the fact that the relative excitation/emission intensities remain constant at a particular concentration of the ion of interest, and are less affected by factors such as unequal dye loading, leakage or photo-bleaching (Malgaroli *et al*., 1987). Thus, unlike conventional fluorescence imaging, ratiometric imaging allows the quantitative detection of absolute or relative changes in ion concentrations within cells.

The earliest ratiometric dyes were developed to measure intracellular $Ca^{2+}$, with Fura-2 and Indo-1 being two of the first reliable dyes developed (Grynkiewicz *et al*., 1985). Subsequently, additional dyes were developed to measure the concentration of other ions, such as $H^+$ with 2',7'-bis-(2'-carboxyethyl)-5',6'-carboxyfluorescein (BCECF) (Graber *et al*., 1986) and carboxy-seminaphthorhodaflour-1 (carboxy-SNARF-1) (Buckler and Vaughan-Jones, 1990), $Na^+$ with sodium-binding benzofuran isophalate (SFBI) (Harootunian *et al*., 1989), and $K^+$ with potassium-binding benzofuran isophalate (PFBI) (Jezek *et al*., 1990). Moreover, advances in genetic manipulation enabled the development of ratiometric imaging techniques such as Förster resonance energy transfer (FRET). The FRET technique involves the construction of synthetic fluorescent proteins with multiple fluorophores, where changes in the protein conformation due to shifts in ion concentration will move the first fluorophore in close proximity to the second and in turn, excite the second fluorophore with the emission of the first fluorophore (Heim and Tsien, 1996). The ratio between the emission intensity of the second and the first fluorophore can be then used in applications such as $Ca^{2+}$ sensing (Miyawaki *et al*., 1997, Truong *et al*., 2001), protein interaction studies (Kenworthy, 2001), and determining cellular localizations of specific proteins (Chen *et al*., 2003, Sekar and Periasamy, 2003).

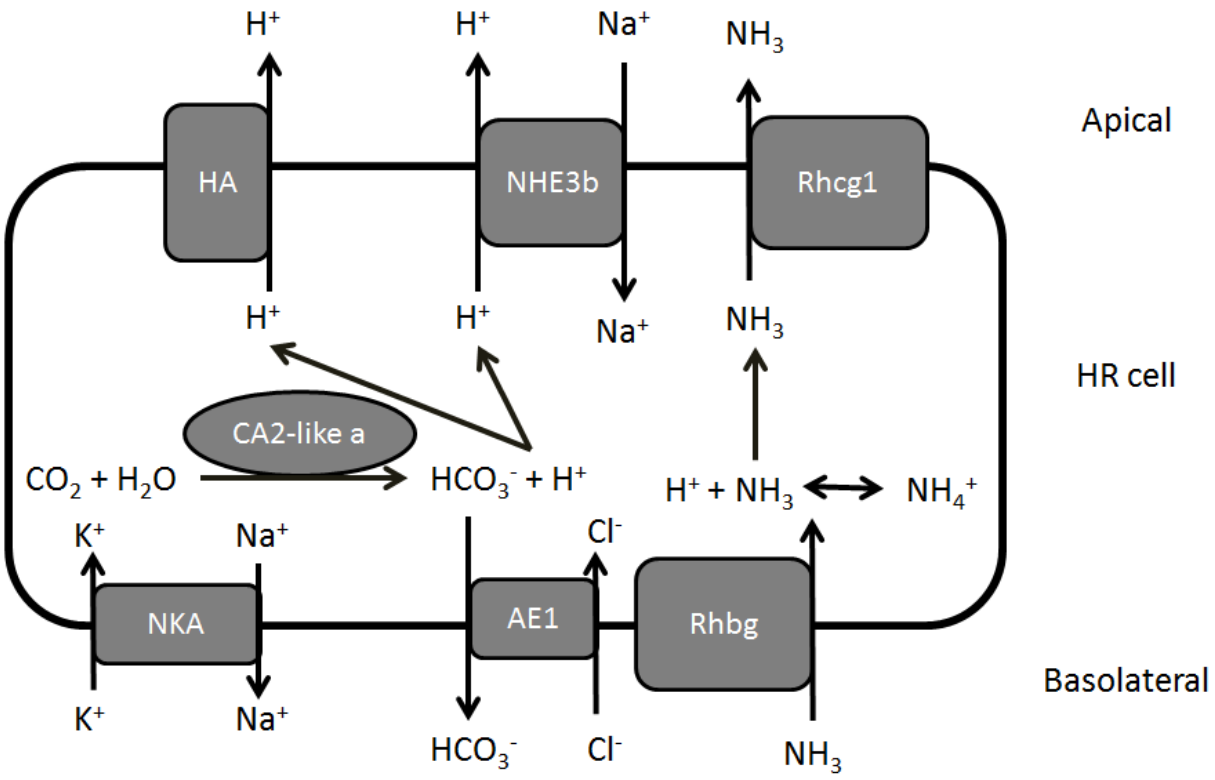
H+
H+
Na+
NH3
Apical
HA
NHE3b
Rhcg1
H+
H+
Na+
NH3
HR cell
CA2-like a
CO2 + H2O
HCO3- + H+
H+ + NH3
NH4+
K+
Na+
Cl-
NKA
AE1
Rhbg
Basolateral
K+
Na+
HCO3-
Cl-
NH3

Fig. 1. Diagram (modified from Hwang and Chou, 2013) illustrating the current model of acid-base regulation in zebrafish HR cells. HA: V-type $H^+$-ATPase; NHE3b: $Na^+/H^+$ exchanger 3b, Rhcg1: Rhesus family, C glycoprotein 1; CA2-like a: Carbonic anhydrase 2-like a; NKA, $Na^+/K^+$ ATPase; AE1: Anion exchanger 1; Rhbg: Rhesus family, B glycoprotein.

## Objectives and Hypothesis

Objectives of thesis

The first goal of this thesis was to develop a method to measure intracellular pH changes in zebrafish larvae HR cells *in vivo*, using ratiometric imaging. The second goal was to assess the role of the various components of HR cell $Na^+$ uptake and $H^+$ extrusion in pHi regulation. The current model of $Na^+$ uptake and $H^+$ extrusion in zebrafish HR cells is well established (Hwang and Chou, 2013) and based predominantly on studies where ion changes were measured from outside the cell or through the whole fish, primarily using techniques such as the scanning ion-selective electrode technique (SIET) (Horng *et al*., 2007, Chang *et al*., 2009, Lee *et al*., 2011) and radioisotopic ion flux studies (Lin *et al*., 2008, Kumai and Perry, 2011, Lee *et al*., 2011). As described earlier in the introduction, the current model stipulates that acid/base regulation is closely tied to $Na^+$ uptake function, and acid secretion is conducted primarily through apical NHE and HA. $HCO_3^-$ excretion also serves a key role in acid/base regulation, but is handled differently between varying FW fish species (reviewed in Hwang and Chou, 2013). However, no studies have yet assessed the role of the apical membrane acid extrusion mechanisms in pHi regulation. When developed for zebrafish larvae, an *in vivo* ratiometric imaging technique will be enable the monitoring of changes of pHi occurring in HR cells in real time in response to external stimuli with and without selective gene knockdown. This technique will provide entirely new perspectives on zebrafish HR cell function.

To elicit pHi changes within the zebrafish HR cell, I propose to use the classical $CO_2$ exposure and ammonium pre-pulse techniques (Boron and de Weer, 1976). The expectation is that $CO_2$ exposure will result in a rapid intracellular acidosis and the subsequent removal of $CO_2$ will induce a rebound in the form of rapid intracellular alkalisation (Boron and de Weer, 1976).

Conversely, exposure and subsequent removal of high external $NH_4^+$ is expected to induce a rapid intracellular alkalosis and acidosis, respectively. I will establish a consistent degree of acidosis/alkalosis in the HR cells using sham-injected fish and compare the results with data obtained from fish in which key components of the HR cell $H^+$ extrusion pathway are selective removed via gene knockdown.

Hypothesis

To demonstrate that the developed method works in tracking pHi changes in zebrafish HR cells in real time, I expect that the $CO_2$ and ammonia pre-pulse experiments will trigger a pHi response in a manner which is consistent with the observations in the original experiment (Boron and de Weer, 1976). Namely, high external $CO_2$ will trigger an acidosis and its removal will cause alkalosis in zebrafish HR cells, while exposure to high external $NH_4^+$ will have the opposite effect. It is important to note that while the original experiments were conducted on isolated cells (Boron and de Weer, 1976), the proposed experiments will be conducted on the whole larva *in vivo*, where various regulatory and compensatory mechanisms should be taken into account (Hwang and Chou, 2013).

I identified three key target proteins/enzymes to be knocked down in the HR cell; the intracellular CA isoform "CA2-like a", the $Na^+/H^+$ exchanger, and the V-type $H^+$-ATPase (HA). Owing to the presumed role of all three proteins in $H^+$ extrusion in zebrafish HR cells, I hypothesize that in the high external $CO_2$ exposure experiments, the morphant fish will exhibit a greater extent of intracellular acidification and a decrease in the rebound alkalosis in the post-$CO_2$ period. I also predict the effects to be greater in the NHE3b and HA morphants as compared to the "CA2-like a" morphants, owing to their direct role in transporting $H^+$ out of the cell as

opposed to the role of "CA2-like a" in facilitating the provision of $H^+$ via the catalysed hydration of $CO_2$ (Lin *et al*., 2008). On the other hand, with the exception of NHE3b which has been found to be functionally related to the ammonia transporter Rhcg1 (Kumai and Perry, 2011, Shih *et al*., 2012), I do not expect any difference between the morphants and the shams in the degree of alkalosis and subsequent acidosis during the period of exposure to high external $NH_4^+$.

## Materials and Methods

### Zebrafish

Adult zebrafish (*Danio rerio*, Hamilton 1822) were supplied by Big Al's Aquarium Services (Ottawa, ON, Canada), and reared in aerated, flowing, dechloraminated Ottawa tap water at 28$^{o}$C. All fish were fed daily with No. 1 Crumble (Zeigler, Gardners, PA, USA) and subjected to a 14h/10h light/darkness daily cycle. All embryos were obtained using standard breeding procedures (Westerfield, 2000) and reared in incubators at 28$^{o}$C in 50 mL petri dishes containing dechloraminated Ottawa tap water supplemented with 0.05% methylene blue. Water was changed daily and dead embryos were removed. All procedures were performed on 5 days post fertilization (dpf) zebrafish, in accordance with protocols approved by the University of Ottawa Animal Care Committee (BL-226, BL-1700) and in adherence to guidelines set by the Canadian Council of Animal Care (CCAC).

### *In vivo* time lapse ratiometric imaging

Zebrafish larvae were anaesthetised using dechloraminated Ottawa tap water containing 200 mg/L tricaine methanesulfonate (MS-222; Syndel Laboratories, Nanaimo, BC, Canada) containing 20 uM pancuronium bromide (Alomone Labs, Jerusalem, Israel) and 1.05 mM Tris base, adjusted to pH 7.6 with NaOH. Concanavalin A (ConA) was used to specifically label HR cells (Yan *et al*., 2007). Larvae were exposed to conA (50 mg/L)-Alexa Fluor 633 conjugate (Invitrogen, Waltham, MA, USA) and 50 μM BCECF, acetoxymethyl ester (AM) dye (Invitrogen, Waltham, MA, USA) for 25 min at room temperature. Larvae were washed in the initial anaesthetic solution 3X and immobilised inside a 35 mm Petri dish in 1.8% low melting-point agarose (Bioshop, Burlington, ON, Canada) dissolved in the same solution. After allowing

the agarose to solidify for 20 min, the larvae were visualised using a Nikon Eclipse Ni-U upright microscope (Nikon Instruments, Tokyo, Japan) and images were captured using an Andor iXon Ultra EMCCD camera (Andor Technology, Belfast, UK). Larvae were maintained in the anaesthetic solution for an additional 30 min before the start of each experiment.

A gravity-driven continuous flow system was used to deliver various solutions to larvae as appropriate and a vacuum pump was used to maintain a constant volume (and height) of fluid in the Petri dish. For each experiment, the larvae were first exposed to the initial solution for 10 min after which the specific experimental solution (depending on the type of experiment) was delivered to the fish for 30 min. Subsequently, the larvae were re-exposed to the initial solution for 30 min. Throughout the course of the experiment, the flow rate was maintained at approximately 1 mL/min, while the larvae were exposed at 20 sec intervals to a sequence of LED excitation light pulses (438, 513 and 633 nm) using a Lumencor Spectra X light engine (Lumencor, Beaverton, OR, USA). Concurrently, emitted light was collected using a 535/20 nm filter for the first 2 wavelengths and a 700/75 nm for the 633 wavelength. Based on conA staining (Lin et al., 2006) and co-localisation with BCECF, 3 specific HR cells on the yolk sac were designated as the regions of interest (ROIs); an area spatially separated from the larva but still within the field of view, was designated as background ROI. Emission intensity data from the ROIs were obtained from the 438 and 513 nm excitation channels and subtracted from the background intensity; the BCECF emission ratio was calculated by dividing the background corrected 513 nm intensity by the background corrected 438 nm intensity. The survival status of larvae was taken note of before and after each experiment by monitoring heart, and only experiments with surviving larvae at the end of the experiment are included.

Experimental treatments

The experimental solution used for the 10-40 min perfusion phase for each experiment varied as below, depending on the type of experiment to be performed:

1. Control experiments

   For proof of concept control experiments, the same initial anaesthetic solution was used in place of the experimental solution. Essentially, the same solution was being used to perfuse the larvae throughout the entire 70-min experiment.

2. Respiratory acidosis

   For experiments designed to elicit respiratory acidosis, a portion of the initial anaesthetic solution that had been equilibrated with 1% $CO_2$ for 30 min prior to the start of the experiment was used in the perfusion phase for these experiments.

3. Metabolic alkalosis

   For experiments that stimulated metabolic alkalosis, a final concentration of 20 mM $NH_4Cl$ was added to a portion of the initial anaesthetic solution, which was then pH-adjusted to 7.6 using NaOH was used in the perfusion phase for these experiments.

Gene knockdown using antisense oligonucleotide morpholinos

For knockdown experiments, embryos were injected with antisense oligonucleotide morpholinos tagged with carboxyfluorescein (GeneTools, Philomath, OR, USA) at the 1-cell stage. NHE3b (*zslc9a3.2; NM_001113479*) was targeted using a morpholino that splices out exon two (5`-AGCTCAGTGACTGGAAAGAGAAATA-3`) (Kumai and Perry, 2011), while HA (*atpv1aa; BC055130*) (5`-ATCCATCTTGTGTGTTAGAAAACTG-3`) and zCAc (*ca2; NM_199215*) (5′-TCGTATCCCCAGTGGTCAGCCATTC-3′) were knocked down using morpholinos that target

the ATG translational start codons (Horng *et al*., 2007, Lin *et al*., 2008). All morpholinos were prepared in 1x Danieau buffer (58 mM NaCl, 0.7 mM KCl, 0.4 mM $MgSO_4$, 0.6 mM $Ca(NO_3)_2$, 5 mM HEPES; pH 7.6) containing 0.05% Phenol Red; 4 ng of morpholino was injected into each embryo, administered using an injection volume of 1 nL. Embryos were screened for the presence of carboxyfluorescein at 1 dpf and only carboxyfluorescein-positive embryos were used for subsequent experiments.

Reverse transcriptase polymerase chain reaction (RT-PCR)

To verify the knockdown of NHE3b, whole-body mRNA was extracted from pools of 30 larvae at 4 dpf using Trizol (Invitrogen, Waltham, MA, USA) according to manufacturer's specifications. As a splice-blocking morpholino was used for NHE3b, RT-PCR was deemed to be a better choice for knockdown verification, since it can be used to detect errant splice patterns in the mRNA. cDNA was synthesized by treating 1 μg of extracted RNA with DNase (Invitrogen, Waltham, MA, USA) and RevertAid M-MNuLV reverse transcriptase (Fermentas, Burlington, ON, Canada), as per the manufacturer's protocol. PCR primers for NHE3b were forward 5`-TCCTGAAACACCACGATTCA-3` and reverse 5`-ACAGGGTCCACAGCAGACAT-3` (Kumai and Perry, 2011). PCR conditions were as follows: Initial denaturation at $94^0$C for 1 min, followed by 30 cycles of $94^0$C for 30 sec, $58^0$C for 30 sec, and $72^0$C for 1 min and a final extension at $72^0$C for 5 min. Primers for 18S rRNA were used to confirm equal loading (forward primer 5`-GGCGGCGTTATTCCCATGACC-3`; reverse primer 5`-GGTGGTGCCCTTCCGTCAATTC-3`). All PCR products were run on a 1% agarose gel and imaged with a Gel doc system equipped with the Quantity-One 1-D analyzer software (BioRad, Mississauga, ON, Canada).

Western blotting

To verify the knockdown of CA2-like a, protein was extracted from pools of 20 larvae using RIPA buffer (150 mM NaCl, 1% Triton X-100, 0.5% sodium deoxycholate, 0.1% SDS, 50 mM Tris-Cl, 1 mM EDTA, 1 mM phenylmethanesulfonyl fluoride) containing a cocktail of protease inhibitors (Product No. 04693116001, Roche, Mississauga, ON, Canada). Samples are then run on a 10% SDS-PAGE at 200 V and transferred onto a polyvinylidene fluoride (PVDF) membrane (BioRad, Mississauga, ON, Canada), using a Trans-Blot SD Semi-Dry Transfer Cell (BioRad, Mississauga, ON, Canada) running at 25 V for 1 h. The membrane was blocked with 5% skim milk in 0.05% Tween-20 in Tris buffer saline (TBS-T) for 2 h at room temperature, followed by incubation of a custom-made primary antibody specific to CA2-like a ( sequence: GYDKHNGPDKWGL, 1:1000 dilution anti-rabbit) in 2% skim milk in 0.05% TBS-T, at 4°C overnight. After washing with 0.05% TBS-T 3 X for 5 min each, the membrane was incubated with an horse radish peroxidase (HRP)-conjugated goat anti-rabbit secondary antibody (1:5000 dilution) (Product No.65-6120, Invitrogen, Waltham, MA, USA) in 2% skim milk in 0.05% TBS-T for 1 h at room temperature. Membranes were then washed 5 X for 5 min each and bands were visualised using enhanced chemiluminescence (SuperSignal West Femto chemiluminescent substrate, Pierce Biotechnology, Waltham, MA, USA) a XRS+ ChemiDoc system (BioRad, Mississauga, ON, Canada). The membrane was then re-probed using a monoclonal β-actin antibody raised in mouse (Product No. A3854, Sigma, St Louis, MO, USA) at 1:4000 dilution after being stripped with ReBlot Plus antibody stripping solution (Millipore, Billerica, MA, USA) according to the manufacturer's specifications.

Whole-mount immunohistochemistry

To verify the knockdown of HA, larvae were exposed to the conA-Alexa Fluor 633 conjugate (50 μg/mL; Invitrogen, Waltham, MA, USA) for 25 min at room temperature and fixed using 4% paraformaldehyde (PFA) in 0.1% Tween-20 in PBS-T, followed by a stepwise dehydration in 100% MeOH in three 5-minute washing steps. After a stepwise rehydration in 0.1% PBS-T in three 5-minute washing steps, larvae were incubated at room temperature with a solution of 3% BSA containing 0.8% Triton X-100 in 0.1% PBS-T for 1 h. Immediately afterwards, larvae were incubated overnight at 4$^{o}$C with a primary antibody specific to a region of the A subunit of bovine HA (AEMPADSGYPAYLGAR, 1:4000 dilution, first used in Ura *et al*., 1996; antibody obtained from Professor Minoru Ushiyama, 100% sequence identity with zebrafish, rabbit host) in 0.3% BSA, 0.8% Trion X-100 in 0.1% PBS-T (Kwong and Perry, 2015). Larvae were rinsed with 3 X and incubated in donkey anti-rabbit secondary antibody conjugated with Alexa Fluor 568 (1:500 dilution) in 0.3% BSA, 0.8% Triton X-100 in 0.1% PBS-T. After 5 washes of 5 min each with 0.1% PBS-T, larvae were mounted on concave glass slides, which were observed and images captured using an A1R+ confocal Microscope (Nikon Instruments, Tokyo, Japan). Solid state lasers emitting at 561 and 633 nm were used for excitation of fluorophores, and images were composed using maximum intensity projection of Z-stacks of 30 μm thickness composed of 30 optical sections of 1 μm each.

Statistical analysis

For each experiment, data were obtained from 3 cells from a single larvae and averaged to yield N = 1. For graphing and statistical purposes, a reference ratio value was determined for each cell; using the average of 10 data points (representing a total of 20 x 10 = 200 sec) before (and including) the point at the 10-min mark of each experiment, each ROI was normalised to a value of 1. Relative normalised ratio data were calculated for all time points prior to and following this reference period by subtracting the reference ratio.

To calculate the maximum normalised ratio change during and after each 30-min experimental treatment (see below), each 20-second ratio measurement interval was averaged with the next 9 ratio measurements to obtain a series of average ratio values, spanning a total interval of 3 min for each measurement. For acidosis experiments, the minimum average ratio value during the 10-40 min period of exposure to $CO_2$ and the maximum average ratio value for the 40-70 min post-$CO_2$ periods were selected. Conversely, for alkalosis experiments the maximum average ratio value during the 10-40 min period of exposure to $NH_4Cl$ and the minimum average ratio value for the 40-70 min post- $NH_4Cl$ periods were selected. For the control group in the proof of concept experiments, the average ratio values at the 40 min and 70 min time points were chosen instead, since the pH value was supposed to remain relatively constant throughout the experiment and no maximum/minimum points reflective of pHi changes was expected. The significance of the difference between these points was assessed within each experiment using one way repeated measurements analysis of variance (ANOVA) and the Holm-Sidak test for comparisons between sets. Additionally, for morphant versus sham experiments, the maximum differences between the points were compared between morphant and sham

experiment sets (10-40 min, 40-70 min and 10-70 min), using Student's t-tests. All p-values < 0.05 were reported as statistically significant.

Also, for the sham vs morphant experiments, the time points during which the BCECF 513/438 value reaches its minimum/maximum during the perfusion and the post-perfusion phases respectively for the $CO_2$ perfusion experiments were recorded individually. Conversely, the maximum/minimum time points of the perfusion and post-perfusion phase were selected for the $NH_4Cl$ experiments. The values of the shams and morphants were compared with each other using a t-test to test for statistical significance. All p-values <0.05 were reported as statistically significant.

## Results

Proof of principle experiments

To specifically monitor relative pHi changes in HR cells, regions of interest (cells) were selected based on co-localization of ConA and BCECF staining (Fig. 2A). To demonstrate that the newly developed ratiometric imaging technique was capable of measuring relative pHi changes in live zebrafish larvae HR cells, a series of experiments was conducted to demonstrate that the BCECF 513/438 ratio was a reliable indicator of relative changes in pHi of HR cells during acute experimental manipulations. The control fish bathed continually with flowing aerated anaesthetic solution did not display a significant change in BCECF 513/438 ratio values during 70 min of recording (Fig. 2B). Exposure of fish to hypercapnia (1% $CO_2$), a treatment expected to induce intracellular acidosis, caused a significant decrease in the BCECF 513/438 ratio which appeared to be reduced maximally after 30 min of treatment (Fig. 2C). Restoration of normocapnia caused the BCECF 513/438 ratio to return to baseline values within 30 min (Fig. 2B). The exposure fish to 20 mM $NH_4Cl$, a treatment known to induce intracellular alkalization, was accompanied by a significant increase in the BCECF 513/438 ratio which was followed by a significant decrease below baseline levels 30 min after the $NH_4Cl$ was washed out (Fig. 2D).

Effects of "CA2-like a" knock down on $CO_2$-induced acidosis and $NH_4^+$-induced alkalosis

Antisense morpholinos targeting "CA2-like a" were used to investigate its role in regulating HR cell pHi in the face of acute acidosis or alkalosis. To confirm that the expression of "CA2-like a" was indeed suppressed in the morphants as previously reported (Miller et al., 2014), qualitative western blot analysis was performed. Representative western blots for β-actin and "CA2-like a"

are depicted in Fig. 3A. There was a clear elimination of the band at ~30 kDa corresponding to the expected molecular weight of "CA2-like a"; the intensity of the β-actin bands was similar.

The fish exposed to 1% $CO_2$ exhibited significant acidosis (decrease in the BCECF 513/438 emission ratio) and a subsequent increase in the BCECF 513/438 emission ratio in the sham and morphant fish when 1% $CO_2$ was removed (Fig. 3B). However, there were obvious temporal and response magnitude differences between the morphant and sham fish. For example the sham fish attained a maximal reduction in the BCECF 513/438 emission ratio only at 27.46 +/- 1.01 min, after which it remained stable, compared to 38.69 +/- 0.69 min in the morphants (Fig. 3B). Although the extent of the BCECF 513/438 emission ratio reduction during the period of $CO_2$ exposure was not statistically different between the sham and morphant fish (Fig. 3C; $p = 0.11$), the extent of the BCECF 513/438 emission ratio recovery upon removal of $CO_2$ was significantly reduced in the morphants (Fig. 3C). The sham fish did not exhibit a return to baseline pHi at a rate significantly different compared to the "CA2-like a" morphant fish (Fig. 3B), but the morphants exhibited a larger net change in the BCECF 513/438 emission ratio compared to shams (Fig 3C). These data indicate a significantly reduced capacity of "CA2-like a" morphants to regulate pHi during and after acute hypercapnia.

During exposure to 20 mM $NH_4Cl$, the time course and extent of intracellular alkalization (increase in the BCECF 513/438 emission ratio) were similar in shams and "CA2-like a" morphants Fig 3D. However, unlike in the sham fish, the HR cells of the "CA2-like a" morphants did not overshoot baseline pHi (i.e. experience relative acidification) within 30 min after the washout of $NH_4Cl$ (Fig. 3D). Indeed, the extent of the BCECF 513/438 emission ratio decrease during the 30 min after $NH_4Cl$ washout was significantly reduced ($P < 0.05$; one-tailed t-test). The time required for sham and morphant fish to reach the maximum point during

perfusion and the minimum point during post-perfusion were not significantly different as well (Fig. 3D).

Effects of NHE3b knock down on $CO_2$-induced acidosis and $NH_4^+$-induced alkalosis

RT-PCR was used to demonstrate the success of NHE3b knock down; the representative gel image (Fig. 4A) indicates a clear reduction of the intensity of the band of interest at 700 bp, while the band intensities for 18S mRNA in NHE3b morphants and sham controls remained constant (Fig. 4A).

Similar to the sham control fish, the HR cells in NHE3b morphants displayed a significant decrease in the BCECF 513/438 emission ratio during the 30 min phase of $CO_2$ exposure and a significant increase in BCECF 513/438 emission ratio during subsequent return to normocapnic conditions (Fig. 4B). However, similar to the "CA2-like a" morphants, the BCECF 513/438 emission ratio in the NHE3b morphants declined continually throughout the period of $CO_2$ exposure until 37.86 +/- 0.56 min, which is significantly longer compared to that of shams at 29.22 +/- 1.15 min (Fig. 4B). The morphants also decreased to a greater extent after 30 min (-0.096 +/- 0.009 in the shams versus -0.198 +/- 0.032 in the NHE3b morphants; Fig. 4C). Additionally, upon return to normocapnia, the extent of the BCECF 513/438 emission ratio recovery (alkalization) was significantly blunted in the NHE3b morphants (Fig. 4B, C). Over the course of the entire 60 min experiment, the NHE3b morphants underwent a net decrease in the BCECF 513/438 emission ratio whereas the shams underwent a net increase in the BCECF 513/438 emission ratio (Fig 4B); after 70 min, the BCECF emission ratios in the morphants and shams had diverged, with the net difference being +0.093 +/- 0.036 in shams and -0.113 +/- 0.035 in NHE3b morphants, Fig. 4C). Additionally, the BCECF emission ratio of morphant fish

(56.42 +/- 2.70 min) plateaued significantly earlier compared to the sham fish (63.67 +/- 1.75 min; Fig. 4C)

The extent of intracellular alkalization during $NH_4Cl$ exposure and relative intracellular acidification during the $NH_4Cl$ washout phase were similar in the sham and NHE3b morphant fish (Fig. 4D, E). It is to note that while the BCECF emission ratio of NHE3b morphants after $NH_4Cl$ washout (between 40-70 min) did not appear to be significantly different from the baseline (Fig. 4D), statistical analysis by one way repeated measures ANOVA using the Holm-Sidak comparison between groups yielded a p-value of 0.038 between the BCECF emission ratios of the baseline and the point after $NH_4Cl$ washout, showing that the difference was indeed significant. Similar to that in the "CA2-like a" morphants, NHE3b morphants did not display any significant difference from the shams in the required to reach the maximum point during perfusion and the minimum point during post-perfusion (Fig. 4D).

Effects of HA knock down on $CO_2$-induced acidosis and $NH_4^+$-induced alkalosis

Immunohistochemistry was used to demonstrate the successful knockdown of HA in the morphants. The representative images depicted in Fig. 5 clearly illustrate abundant expression of HA in the ConA-positive HR cells (Fig 5A) of shams which was absent in the ConA-positive HR cells of the morphants (Fig. 5B).

The exposure of fish to 1% $CO_2$ and their subsequent return to normocapnic conditions revealed two significant differences between the HA and the previous two morphants. First, the maximal absolute intracellular acidification achieved within 30 min (i.e. the decreases in the BCECF 513/438 emission ratios of $CO_2$ exposure) did not differ significantly between the

morphants and the shams (Fig. 5D), and the pHi of HR cells in the morphants stabilized at the 35.56 +/- 2.66 min time point, which was not significantly different from the sham fish at 31.83 +/- 0.90 min (Fig. 5C). Secondly, while the morphants did not exhibit a significantly different amount of recovery of the BCECF 513/438 emission ratio from the sham fish during post-$CO_2$ recovery, there was, however, a significant difference in the extent of the pHi change (BCECF 513/438 emission ratios) between the shams and morphants at the conclusion of the experiments (Fig. 5D).

For the $NH_4Cl$ experiments, the HR cells from both HA morphants and shams exhibited a significant increase in BCECF 513/438 ratio during the 30 min exposure phase and a significant decrease in BCECF 513/438 ratio during the period following its washout (Fig. 5E). There were no difference in the time courses or extent of intracellular pH changes between the shams and morphants (Fig. 5E, F).

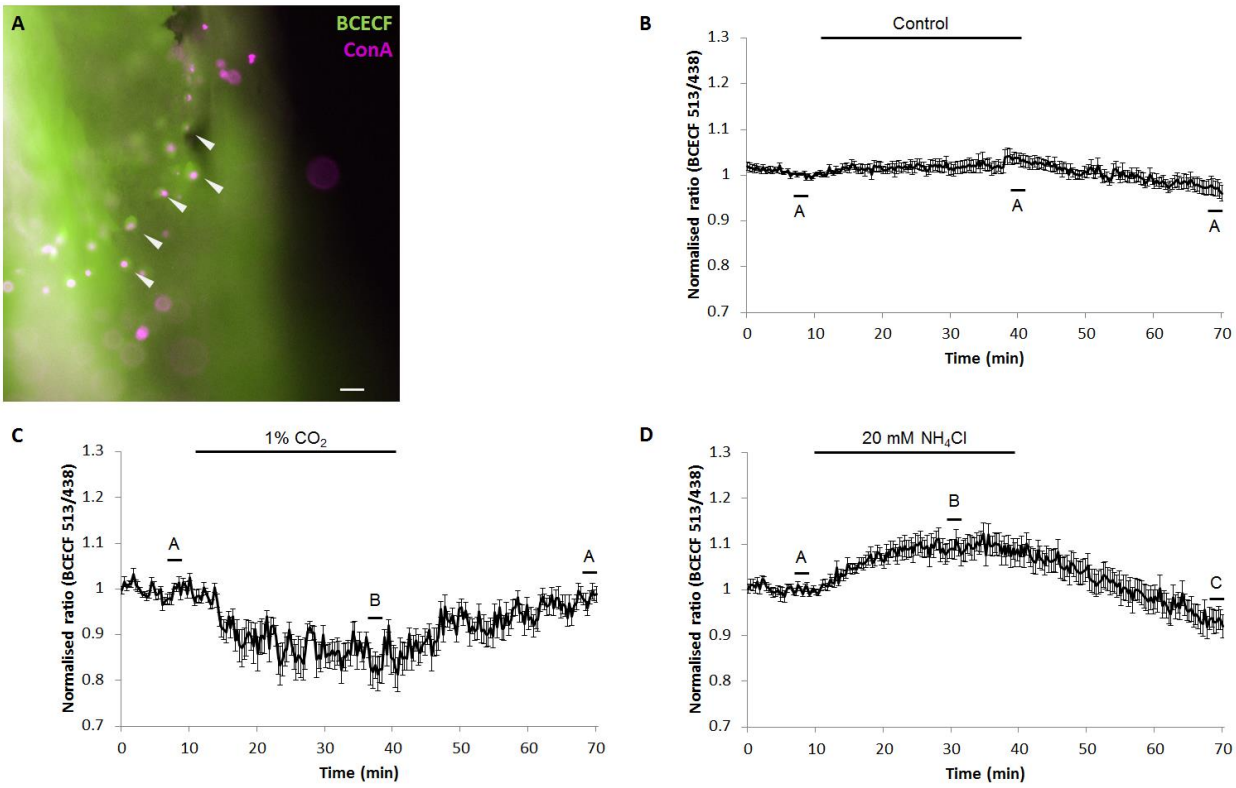
A
BCECF
ConA
B
Control
Normalised ratio (BCECF 513/438)
Time (min)
A
A
A
C
1% CO2
Normalised ratio (BCECF 513/438)
Time (min)
A
B
A
D
20 mM NH4Cl
Normalised ratio (BCECF 513/438)
Time (min)
A
B
C

Fig. 2. *In vivo* ratiometric imaging of HR cells on the yolk sac epithelium of 5 dpf zebrafish larvae using the pH indicator BCECF. Cells targeted for imaging were selected based on co-localization of BCECF and the HR cell marker Concanavalin A (ConA; white arrowheads) (A). Scale bar at bottom-right corner indicates a distance of 20 μm (A). Larvae were bathed initially with flowing aerated water containing anaesthetic followed either by continued delivery of aerated water (B) or exposure to 1% $CO_2$- (C; N = 4) or 20 mM $NH_4Cl$-enriched water (D; N = 8). Horizontal lines above the graphs indicate the durations of $CO_2$ or $NH_4Cl$ exposures. Changes in the BCECF 513-438 emission ratio correlate positively to changes in pHi. The 3 reference points in each graph indicate the baseline, averaged maximum/minimum emission ratios during the treatment period (10 - 40 min) and the averaged maximum/minimum ratios during the post-treatment period (40 - 70 min). Different letters indicate a significant difference between the points within the same data sets ($p < 0.05$).

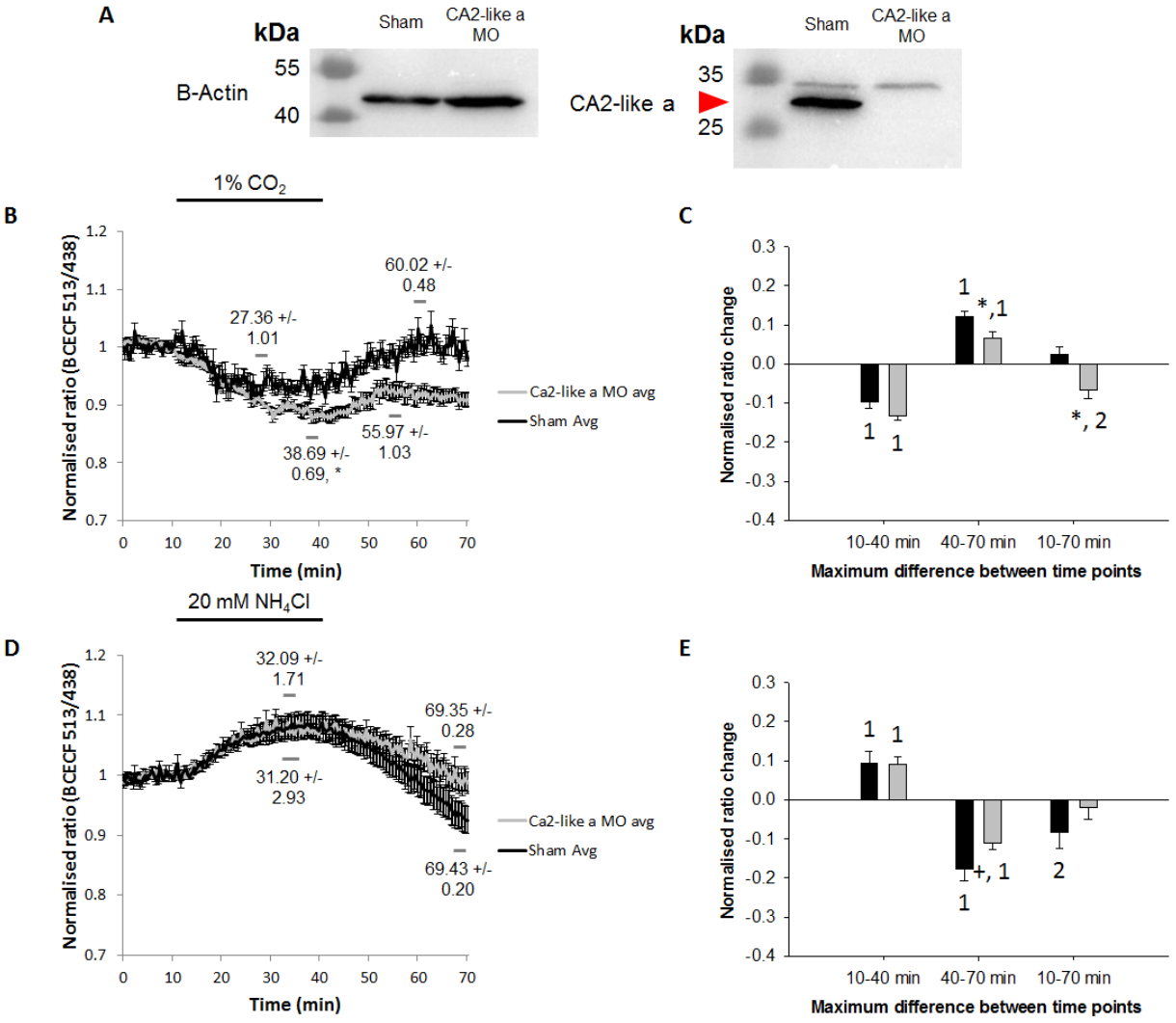
A
kDa
Sham
CA2-like a MO
55
40
B-Actin
kDa
Sham
CA2-like a MO
35
25
CA2-like a
B
1% CO2
Normalised ratio (BCECF 513/438)
60.02 +/- 0.48
27.36 +/- 1.01
55.97 +/- 1.03
38.69 +/- 0.69, *
Ca2-like a MO avg
Sham Avg
Time (min)
C
Normalised ratio change
1
*,1
1
1
*, 2
10-40 min
40-70 min
10-70 min
Maximum difference between time points
D
20 mM NH4Cl
Normalised ratio (BCECF 513/438)
32.09 +/- 1.71
69.35 +/- 0.28
31.20 +/- 2.93
69.43 +/- 0.20
Ca2-like a MO avg
Sham Avg
Time (min)
E
Normalised ratio change
1
1
1
+, 1
2
10-40 min
40-70 min
10-70 min
Maximum difference between time points

Fig. 3. The effects of "CA2-like a" knockdown on relative intracellular pH changes (monitored using *in vivo* BCECF ratiometric imaging) in HR cells of 5 dpf zebrafish larvae subjected to respiratory acidosis or metabolic alkalosis. Fish were injected with "CA2-like a" or sham morpholinos (MO) at the 1-cell stage. The representative western blot (A) illustrating the absence of CA2-like a protein (red arrowhead) in the morphant fish demonstrates the effectiveness of knockdown. After 10-min of baseline recording, fish were exposed for 30 min to either 1% $CO_2$ (B, C; N = 4) or 20 mM $NH_4Cl$ (D, E; N = 6). Bars above graphs (B, D) indicate the 30 min periods of exposure to $CO_2$ or $NH_4Cl$. Changes in the BCECF 513/438 emission ratio correlate positively to changes in pHi. The 3 reference points in each graph (B, D) indicate the baseline, averaged maximum/minimum emission ratios during the treatment period (10 - 40 min) and the averaged maximum/minimum ratios during the post-treatment period (40 - 70 min). Numbers indicated on each point refer to the averages +/- standard errors of each the corresponding time points chosen. Bar graphs illustrate the changes in normalised BCECF 513/438 ratios between the indicated reference points within the specified time periods (C, E). Asterisks indicate $p < 0.05$ (two-tailed Student's t-test) and crosses indicate $p < 0.05$ (one-tailed t-test) that the values of the morphants are significantly different from shams. The number 1 on the bar graphs represents $p<0.05$ (two-tailed Student's t-test) while the number 2 represents $p<0.05$ (one-tailed t-test) that the ratio change is significantly different from 0.

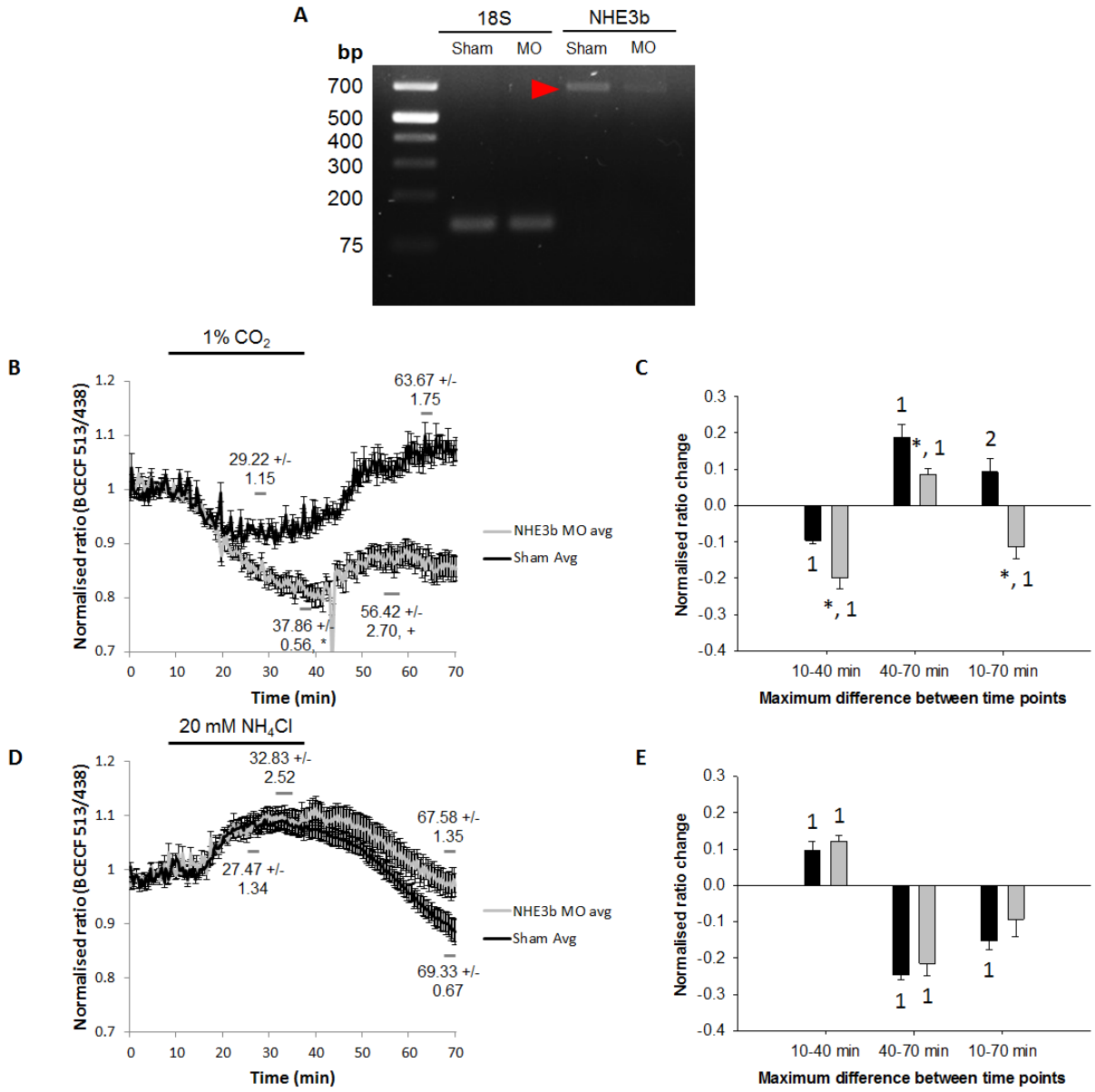
A
18S
NHE3b
Sham
MO
Sham
MO
bp
700
500
400
300
200
75
B
1% CO2
63.67 +/- 1.75
29.22 +/- 1.15
37.86 +/- 0.56, *
56.42 +/- 2.70, +
NHE3b MO avg
Sham Avg
Normalised ratio (BCECF 513/438)
Time (min)
C
Normalised ratio change
1
*, 1
2
1
*, 1
*, 1
10-40 min
40-70 min
10-70 min
Maximum difference between time points
D
20 mM NH4Cl
32.83 +/- 2.52
67.58 +/- 1.35
27.47 +/- 1.34
69.33 +/- 0.67
NHE3b MO avg
Sham Avg
Normalised ratio (BCECF 513/438)
Time (min)
E
Normalised ratio change
1
1
1
1
1
10-40 min
40-70 min
10-70 min
Maximum difference between time points

Fig. 4. The effects of NHE3b knockdown on relative intracellular pH changes (monitored using *in vivo* BCECF ratiometric imaging) in HR cells of 5 dpf zebrafish larvae subjected to respiratory acidosis or metabolic alkalosis. Fish were injected with NHE3b or sham morpholinos (MO) at the 1-cell stage. The representative RT-PCR gel (A) illustrating the absence of the 700 kDa PCR product (red arrowhead) in the morphant fish demonstrates the effectiveness of knockdown. After 10-min of baseline recording, fish were exposed for 30 min to either 1% $CO_2$ (B, C; N = 4) or 20 mM $NH_4Cl$ (D, E; N = 4). Bars above graphs (B, D) indicate the 30 min periods of exposure to $CO_2$ or $NH_4Cl$. Changes in the BCECF 513/438 emission ratio correlate positively to changes in pHi. The 3 reference points in each graph (B, D) indicate the baseline, averaged maximum/minimum emission ratios during the treatment period (10 - 40 min) and the averaged maximum/minimum ratios during the post-treatment period (40 - 70 min). Numbers indicated on each point refer to the averages +/- standard errors of each the corresponding time points chosen. Bar graphs illustrate the changes in normalised BCECF 513/438 ratios between the indicated reference points within the specified time periods (C, E). Asterisks indicate $p < 0.05$ (two-tailed Student's t-test) and crosses indicate $p < 0.05$ (one-tailed t-test) that the values of the morphants are significantly different from shams. The number 1 on the bar graphs represents $p<0.05$ (two-tailed Student's t-test) while the number 2 represents $p<0.05$ (one-tailed t-test) that the ratio change is significantly different from 0.

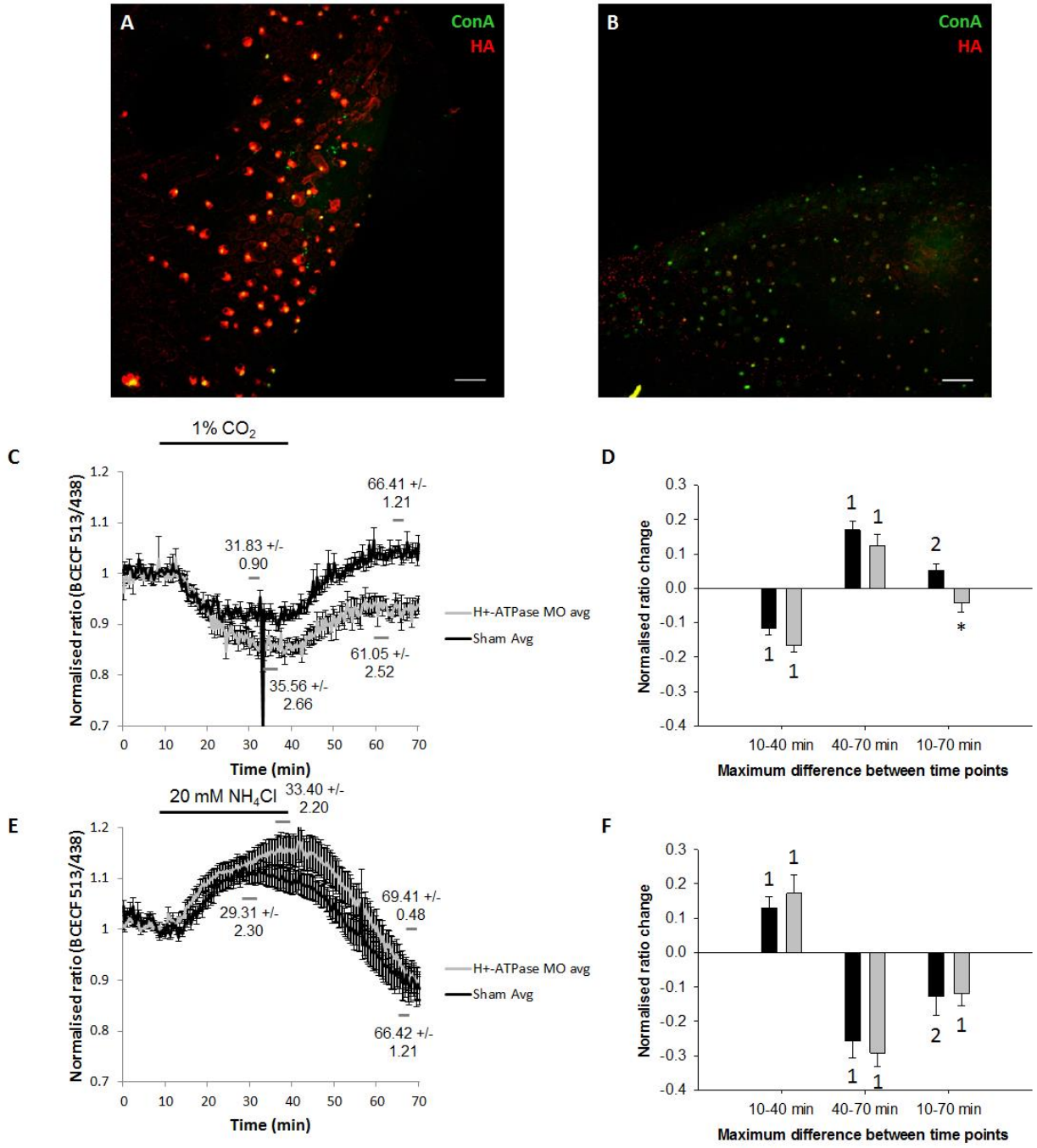
A
ConA
HA
B
ConA
HA
C
1% $CO_2$
Normalised ratio (BCECF 513/438)
66.41 +/- 1.21
31.83 +/- 0.90
61.05 +/- 2.52
35.56 +/- 2.66
H+-ATPase MO avg
Sham Avg
Time (min)
D
Normalised ratio change
10-40 min
40-70 min
10-70 min
Maximum difference between time points
E
20 mM $NH_4Cl$
33.40 +/- 2.20
29.31 +/- 2.30
69.41 +/- 0.48
66.42 +/- 1.21
Normalised ratio (BCECF 513/438)
H+-ATPase MO avg
Sham Avg
Time (min)
F
Normalised ratio change
10-40 min
40-70 min
10-70 min
Maximum difference between time points

Fig. 5. The effects of $H^+$-ATPase (HA) knockdown on relative intracellular pH changes (monitored using *in vivo* BCECF ratiometric imaging) in HR cells of 5 dpf zebrafish larvae subjected to respiratory acidosis or metabolic alkalosis. Fish were injected with HA or sham morpholinos (MO) at the 1-cell stage. The representative whole mount immunohistochemistry images, showing the presence (A) or absence (B) of co-localization between ConA and HA staining in sham and HA morphants illustrates the effectiveness of knockdown. After 10-min of baseline recording, fish were exposed for 30 min to either 1% $CO_2$ (B, C; N = 4) or 20 mM $NH_4Cl$ (D, E; N = 6). Bars above graphs (B, D) indicate the 30 min periods of exposure to $CO_2$ or $NH_4Cl$. Changes in the BCECF 513/438 emission ratio correlate positively to changes in pHi. The 3 reference points in each graph (B, D) indicate the baseline, averaged maximum/minimum emission ratios during the treatment period (10 - 40 min) and the averaged maximum/minimum ratios during the post-treatment period (40 - 70 min). Numbers indicated on each point refer to the averages +/- standard errors of each the corresponding time points chosen. Bar graphs illustrate the changes in normalised BCECF 513/438 ratios between the indicated reference points within the specified time periods (C, E). Asterisks indicate $p < 0.05$ (two-tailed Student's t-test) that the values of the morphants are significantly different from shams. The number 1 on the bar graphs represents $p<0.05$ (two-tailed Student's t-test) while the number 2 represents $p<0.05$ (one-tailed t-test) that the ratio change is significantly different from 0.

## Discussion

To our knowledge, only one previous study successfully monitored relative pHi changes *in vivo* and in real time in any animal species. The previous study (Mölich and Heisler, 2005) was conducted by direct injection of the SNARF-1 ratiometric dye into zebrafish embryos at a very early developmental stage and fish were monitored only until the end of epiboly (~10 h post fertilisation). For the current study, a subtype of zebrafish ionocyte, the HR cell, was targeted because of the wealth of existing data surrounding its $H^+$ excretory pathways and its straightforward identification *in vivo* using the vital fluorescently-tagged HR cell marker, concanavalin A. The principal novel finding of the present study is that three components of the $Na^+$ uptake/$H^+$ extrusion pathway contribute to regulation of HR intracellular respiratory acidosis; namely the catalysed production of $H^+$ from $CO_2$ via "CA2-like a", $Na^+/H^+$ exchange via NHE3b and active $H^+$ secretion via V-type $H^+$-ATPase. Yet, none of these pathways appear to contribute significantly to regulation of HR intracellular alkalosis aside from a small contribution from "CA2-like a".

### A critique of the methods and analytical procedures

A notable feature and obvious limitation of the current study is that all data are presented as BCECF 513/438 emission ratios, rather than absolute pHi values. The absence of absolute pHi results in the current study reflects an inability to obtain meaningful *in vivo* calibration data whereby BCECF 513/438 emission ratios can be converted to specific pHi values. In brief, we were unsuccessful in applying *in situ* pHi calibration techniques previously validated for cell cultures and used successfully in our earlier studies with isolated cells (e.g. Furimsky *et al*., 1999). Two standard calibration methods were attempted; exposure to the $K^+/H^+$ ionophore

nigericin in the presence of high [$K^+$] (Montrose *et al*., 1986) or exposure to the $H^+$ ionophore carbonyl cyanide m-chlorophenyl hydrazine (CCCP) (James-Kracke, 1992). In both cases, the larvae did not survive long enough for pHi calibrations to be conducted when using the required concentrations of the reagents. Additionally, we attempted to convert BCECF 513/438 emission data to absolute pHi values using an *in vitro* calibration procedure. Although this technique has been employed successfully for cell cultures (Boyarski *et al*., 1996), applying the method to living larvae presented a unique set of problems. In our experiments, care must be taken to select the ROIs on HR cells in a similar region of the larvae with minimal yolk sac auto fluorescence, a phenomenon previously observed in zebrafish larvae when recording emission data near wavelengths required for BCECF visualisation (McGinty *et al*., 2011). However, despite the careful selection of ROIs, in practice the background fluorescence was still sufficient to influence the pHi conversions to values which were far from expected pHi ranges for fish cells (Furimsky *et al*., 1999). Additionally, owing to the varying BCECF 513/438 ratio values between individual experiments, the calibrations would need to be conducted on an experiment-by-experiment basis, which is cost prohibitive because of the large quantities of BCECF required for each calibration (BCECF must be added to the flowing extracellular media).

Additionally, I chose to present the BCECF 513/438 ratios in a form normalised to the baseline ratio values of each individual experiment, instead of presenting the raw BCECF 513/438 ratio values. As mentioned earlier, BCECF 513/438 ratio values vary substantially between individual experiments. Thus, although the microscope settings and experimental parameters remained constant between experiments, slight differences in other factors such as yolk sac auto fluorescence, relative positioning of HR cells and gel thickness can cause variations in the acquired BCECF 513/438 ratios, even when recording from multiple cells from

the same larva. Because HR cells are expected to exhibit a consistent and narrow pHi range when exposed to similar conditions, the normalised ratio values are more useful in capturing the relative changes of pHi in the cells exposed to acid-base challenges. Perhaps, the greatest limitation of this normalisation procedure is the inability to assess whether HR absolute pHi is changing with the gene knockdown treatments. Regardless, in the absence of a suitable calibration technique, the data must be presented in a normalised manner.

Proof of principle experiments

Given that the BCECF emission ratios could not be converted to absolute pHi data, it was critical to demonstrate that HR cells exposed to respiratory acidosis (1% $CO_2$) or metabolic alkalosis (20 mM $NH_4Cl$) exhibited BCECF 513/438 emission ratios indicative of the pHi changes expected to accompany such treatments. Thus, considering that decreases and increases in BCECF 513/438 emission ratios are known to represent intracellular acidification and alkalisation, respectively, it was predicted that exposure to 1% $CO_2$ would yield a fall in BCECF 513/438 emission ratios while exposure to $NH_4Cl$ would cause an increase in the ratio. Furthermore, the washout of $CO_2$ and $NH_4Cl$ were expected to elicit abrupt reversals of the BCECF ratios. Indeed, these patterns of BCECF 513/438 emission ratio changes were observed consistently in preliminary experiments (Fig. 2). Moreover, the washout of $NH_4Cl$ was associated with a decrease (undershoot) in HR BCECF 513/438 emission ratios below baseline values indicative of cellular acidification related to compensatory accumulation of $H^+$ equivalents during the phase of alkalisation. It was also expected that compensatory excretion of $H^+$ equivalents during the $CO_2$-induced intracellular acidification would be reflected by an increase in the BCECF 513/438 ratio above baseline upon return to normocapnic conditions. Interestingly, this phenomenon was

observed in control (sham-injected) fish in half of the experiments only (see below; Figs. 4 and 5).

For the remainder of the discussion, we have assumed that a decrease in the BCECF 513/438 emission ratio is indicative of a fall in pHi whereas an increase in the ratio represents an increase in pHi. Thus, hereafter we refer to intracellular pH changes rather than changes in the BCECF 513/438 emission ratios.

pHi regulation in zebrafish HR cells during and after $CO_2$-induced acidosis

Boron and De Weer (1976) described in detail the changes in pHi in squid giant axons exposed to 5% $CO_2$ and subsequently returned to normocapnia. The complex changes in pHi described by Boron and De Weer (1976) and the accompanying cellular mechanisms have subsequently been applied to a multitude of cell types and species including fish gill cells (e.g. Pelster, 2004; Parks *et al*., 2007; 2010) and hepatocytes (e.g. Walsh, 1986). Three phases of pHi changes are typical of cells exposed to, and then removed from, enriched $CO_2$ solutions. First, a phase of rapid acidification occurs, reflecting the diffusive entry of $CO_2$ and its hydration to $HCO_3^-$ and $H^+$. Second, a "plateau phase" is observed, representing a slow increase in pHi despite the continued presence of $CO_2$ which results from compensatory excretion of $H^+$ equivalents via regulated pathways. A third phase accompanies the removal of $CO_2$ which consists of a rapid alkalisation which may overshoot baseline pHi values. The extent of the overshoot during the rapid re-equilibration of $CO_2$ reflects the quantity of $H^+$ equivalents accumulated during the plateau phase and thus can be used as an index of intracellular acid-base compensation. However, it is important to emphasise that an additional acidification phase of intracellular acid-base adjustment occurs simultaneously with the plateau phase and indeed may even obscure the plateau phase entirely. During this additional phase, the cell continues to acidify slowly after

initial $CO_2$ entry owing to outwardly directed $HCO_3^-$ movements which serve to lower intracellular $PCO_2$ and thus fuel continued entry of $CO_2$ into the cell (the Jacobs-Stewart cycle) (Jacobs and Stewart, 1942). Thus, the net change in pHi during the plateau phase represents the opposing consequences of any compensatory excretion of $H^+$ coupled with the continued entry of $H^+$ via the Jacobs-Stewart cycle.

Given this theoretical framework, we opted to estimate the degree of intracellular acid/base compensation and thus assess the roles of "CA2-like a", NHE3b and HA in pHi regulation by comparing the changes in relative pHi between sham and morphant fish over different phases of each experiment.

The role of "CA2-like a" in regulating intracellular acidosis

The specific cytosolic carbonic anhydrase isoform, "CA2-like a", is abundantly expressed in zebrafish HR cells (Lin et al., 2008) where it is thought to catalyse the hydration reaction of $CO_2$ to yield $H^+$ and $HCO_3^-$ (reviewed by Guh *et al*., 2015). The $H^+$ derived from the catalysed hydration of $CO_2$ is thereby made available to provide substrate for $Na^+/H^+$ exchange via NHE3b and $H^+$ secretion via V-type $H^+$-ATPase (HA). In support of this model, the selective knockdown of "CA2-like a" caused a significant decline in $H^+$ extrusion (as measured by SIET) in zebrafish larvae at 4 dpf (Lin *et al*., 2008). However, the effects of CA knockdown on $H^+$ extrusion were relatively modest (~20%; Fig. 5 in Lin *et al*., 2008) perhaps owing to a simultaneous increase in NHE3b expression (see below). The effect of "CA2-like a" knockdown on decreasing the magnitude of net $H^+$ extrusion was similar to the inhibitory effect of NHE3b knockdown (Shih *et al*., 2012) but much less than the large reduction in $H^+$ secretion associated with HA knockdown (Horng *et al*., 2006).

In the present study, the effects of "CA2-like a" knockdown on intracellular pH regulation during respiratory acidosis were consistent with its role in aiding the provision of $H^+$ for NHE3b and HA. During exposure to $CO_2$, the HR pHi did not stabilise but continued to decrease in the morphants indicating that any compensatory secretion of $H^+$ was unable to match the continuing acidification arising from the Jacobs-Stewart cycle (Fig. 3B). Moreover, upon return to normocapnic conditions, the morphants exhibited a significant blunting of the cellular re-alkalisation phase such that pHi had not returned to baseline after 30 min (Fig. 3B) and thus pHi was significantly lower than in the shams upon termination of the experiment (Fig. 3C). Ultimately, the difference in pHi between the morphants and sham fish at the conclusion of the experiment must reflect the reduced excretion of $H^+$ via NHE3b or HA linked to catalysed hydration of $CO_2$.

Linking CA activity to $Na^+$ uptake and $H^+$ excretion in zebrafish has not proven straightforward. Although "CA2-like a" is believed to function as part of a multi-component transport metabolon with NHE3b and Rhcg1 (Ito *et al*., 2013) and its knockdown reduces the accumulation of $Na^+$ in HR cells (Ito *et al*., 2013), other studies have reported a stimulation of $Na^+$ uptake with "CA2-like a" knockdown in larvae (Lin *et al*., 2008) or adults (Boisen *et al*., 2003). Interestingly, in the study which demonstrated stimulation of $Na^+$ uptake in adult zebrafish with CA inhibition using ethoxzolamide (Boisen *et al*., 2003), the effect was observed only in fish acclimated to soft water ($[Ca^{2+}]$ = 4.4 μM; $Na^+$ = 35 μMM; $Na^+$ = 1480 μM; $[Cl^-]$ = 43 μM) at pH 6.0. In fish acclimated to hard water ($[Ca^{2+}]$ = 3246 μM; $[Cl^-]$ = 1625 μM) at pH 8.2, $Na^+$ uptake was reduced by CA inhibition (Boisen *et al*., 2003). An obvious confounding factor in interpreting the results of studies in which "CA2-like a" is knocked down in zebrafish larvae, is the associated increase in expression of NHE3b and reduced expression of HA (Lin *et*

*al*., 2008). Moreover, it must be stressed that $CO_2$ hydration reactions will continue to proceed relatively quickly even at uncatalysed rates at 28$^{o}$ C (Edsall, 1969). Indeed, it is the slow velocity of the uncatalysed $HCO_3^-$ dehydration reaction that is more often considered to be rate-limiting in biological systems lacking CA activity.

The role of NHE3b and HA in regulating intracellular acidosis

Although previous studies on zebrafish larvae have demonstrated that knockdown of HA reduces $H^+$ excretion to a greater extent than NHE3b knockdown (Horng *et al*., 2006; Lin *et al*., 2008), the results of the present study revealed a greater impact of NHE3b knockdown on pHi regulation suggesting that $Na^+/H^+$ exchange via NHE3b may play a greater role than active $H^+$ secretion via HA in regulating intracellular acidosis (compare Figs. 4 and 5). Although the $Na^+$ and $H^+$ chemical gradients across the apical membrane of HR cells are inconsistent with the function of electroneutral $Na^+/H^+$ exchange (see Parks *et al*., 2008), it is nevertheless clear that NHE3b does in fact contribute to $Na^+$ uptake in zebrafish larvae even under highly unfavourable conditions of low external pH (Kumai *et al*., 2012) or low external [$Na^+$] (Shih *et al*., 2012). Despite the unfavourable macroscopic chemical gradients for $Na^+/H^+$ exchange, it has been proposed that favourable localised gradients across the apical membrane are created via close association of NHE3b with Rhcg1 and "CA2-like a" (Kumai *et al*., 2012; Shih *et al*., 2012; Ito *et al*., 2013). Thus, as proposed by Wright and Wood (2009), the outward diffusive movement of $NH_3$ via Rhcg1and its subsequent protonation to $NH_4^+$ serves to create a localised alkaline environment immediately adjacent to the gill epithelium. The increased pH of the external boundary layer, when coupled with the localised production of $H^+$ from $CO_2$ via "CA2-like a" in

the sub-apical region of HR cells, is thought to thermodynamically enable NHE3b-mediated $Na^+/H^+$ exchange.

Given the proposed model for $Na^+/H^+$ exchange, a possible explanation for the large effect of NHE3b knockdown on pHi regulation during respiratory acidosis is that the large influx of $CO_2$ into the HR cells and the subsequent hydration to $H^+$ and $HCO_3^-$ resulted in a further increase in $[H^+]$ in the HR cells in the vicinity of NHE3b, thus further enabling $Na^+/H^+$ exchange disproportionally over the energy-consuming HA pathway. Further supporting this theory is the "plateau" during $CO_2$-induced acidification occurs significantly later in NHE3b and "CA2-like a" morphants, but not in HA morphants, when compared to shams (Figs. 4 and 5). Regardless, all three morphant groups, including the HA morphants, displayed a significant decrease in pHi change throughout the entire experiment compared to the sham controls. Thus, while NHE3b might be the preferred pathway for $H^+$ extrusion during $CO_2$-induced acidosis, the ATP-driven $H^+$-ATPase still remains a critical component for the long-term recovery of pHi from intracellular acidosis in HR cells.

pHi regulation in zebrafish HR cells during external $NH_4^+$-induced alkalosis

Intracellular alkalosis was induced in HR cells by exposing the larvae to high external ammonia levels (20 mM $NH_4Cl$). In the original study describing the ammonia pre-pulse method (Boron and De Weer, 1976), the intracellular alkalosis was explained by the rapid influx of $NH_3$ into the cell, likely through apical membrane channels permeable to water such as aquaporins (Nakhoul *et al*., 2001). Given the more recent discovery of specific ammonia channels (Rh proteins; Nakada *et al*., 2007), it is more likely that during such experiments, $NH_3$ enters the cell via plasma membrane Rh proteins. In zebrafish HR cells, the expected route of entry is via Rhcg1 (Nakada et al., 2007; Braun et al., 2009). Given the high pKa of the $NH_3$-$NH_4^+$-$H^+$ equilibrium

reaction (~9.25) relative to typical pHi values (6.8 – 7.6 depending on species and developmental age), $NH_3$ will combine with $H^+$ to form $NH_4^+$ thereby raising pHi (Boron and de Weer, 1976). Assuming a similar cause of intracellular alkalosis in zebrafish larvae HR cells during exposure to $NH_4^+$, it was expected that one or both of the apical membrane $H^+$ extrusion pathways (NHE3b or HA) would be inhibited to facilitate $H^+$ accumulation. Interestingly, all fish, regardless of treatment displayed similar increases in pHi during exposure to 20 mM $NH_4Cl$ (Fig. 3E, 4E, 5F) and with the exception of the CA morphants, exhibited equivalent degrees of acidification upon washout of $NH_4Cl$. Indeed, the "CA2-like a" morphants also did not experience a pHi undershoot upon $NH_4Cl$ removal which was consistent with reduced compensatory accumulation of $H^+$ during the period of $NH_4Cl$ exposure.

Although the focus of the current study was on HR apical membrane $H^+$ extrusion pathways, it should be noted that HR cells also are believed to expresses a basolateral $Cl^-/HCO_3^-$ anion exchanger (isoform AE1b; *slc4a1b*) (Lee *et al*., 2011). Thus, it is possible that the major route of compensatory $H^+$ accumulation during $NH_4Cl$ exposure occurs via $HCO_3^-$ excretion in which case the effect of "CA2-like a" knockdown on pHi regulation could be explained by a reduced supply of $HCO_3^-$ for $Cl^-/HCO_3^-$ exchange. The involvement of basolateral anion exchangers in acid-base regulation was demonstrated in type A intercalated cells in mammalian kidneys (Wagner *et al*., 2006). Furthermore, studies on the spotted green pufferfish (*Tetraodon nigrovirids*) have shown that AE1 colocalizes with CA and these proteins are functionally related to each other (Tang and Lee, 2007). Thus, it is possible that the catalysed hydration of $CO_2$ is required to stimulate $HCO_3^-$ excretion across the basolateral membrane via AE1b, which would explain why a significant decrease in post- $NH_4Cl$ acidosis was observed only in "CA2-like a" morphants, but not in NHE3b or HA morphants.

Future directions

The ratiometric imaging technique developed in the current study enables the measurement of pHi changes occurring in real time in individual cells of living zebrafish larvae and will open up new possibilities to study acid-base regulatory mechanisms in HR cells and other ionocyte subtypes.

One specific area which I have been investigating during the course of this thesis is the effects of cortisol on the acid-base regulating capacities of zebrafish larvae HR cells. Recent studies have found that cortisol increases acid secretion and $Na^+$ uptake in zebrafish HR cells (Kumai *et al*., 2012, Lin *et al*., 2015). In addition, exposure to cortisol increases the number of HR cells in larvae by regulating transcription factors required for the development of HR cells (Cruz *et al*., 2013). It would be interesting to see whether the increased $H^+$ extrusion capacity translates to an increased ability to regulate pHi in HR cells, and to see how HR cells of cortisol-treated larvae respond to externally induced changes to pHi. I have gathered some preliminary data on the subject but have yet to acquire sufficient data to reach firm conclusions.

A potential future experiment is to treat zebrafish larvae with other hormones which are known to affect acid-base regulation. Catecholamines have been shown to regulate $Na^+$ uptake in HR cells through the cyclic AMP pathway (Kumai *et al*., 2014). Endothelin-1 is known to increase $H^+$-ATPase dependent acid secretion in HR cells in a cell-specific manner (Guh *et al*., 2014). Also, there are some other potential protein/enzyme candidates worth investigating, which are also involved in acid/base regulation in HR cells. Some examples include the extracellular

carbonic anhydrase isoform CA15a (Lin *et al*., 2008), the ammonia transporter Rhcg1 (Kumai and Perry, 2011) and the basolateral $Cl^-/HCO_3^-$ exchanger AE1b (Lee *et al*., 2011).

Further applications of the *in vivo* ratiometric imaging technique

Currently, a major limitation with the in vivo ratiometric pHi imaging technique is the inability to measure absolute *in vivo* pHi values. Our previous attempts to calibrate pHi using the $K^+$/nigericin and carbonyl cyanide m-chlorophenyl hydrazone (CCCP) calibration methods all resulted in the death of the larvae when exposed to the necessary $K^+$ or CCCP concentrations respectively. Also, the widely varying absolute 513/438 emission ratio values between individual experiments render *in vitro* calibrations unfeasible. In the near future, we hope to explore or even develop other calibration methods, to allow the measurement of absolute pHi values in cells of interest in a consistent and reproducible manner. The creation of a method to calibrate the pHi of cells of zebrafish larvae while keeping the larvae alive is of utmost importance.

Although currently we are able only to localize BCECF staining to HR cells (Fig. 2D), by making slight adjustments to the staining protocol and using other vital cell markers, I hope that this new method can be used to conduct time lapse imaging in other ionocyte cell types, such as NaR and NCC cells. In addition, it may be possible to use other ratiometric dyes to measure the concentration of other ions such as $Ca^{2+}$ and $Na^+$ in intracellular environments. This was demonstrated by a very recent study conducting *in vivo* measurements of intracellular [$Na^+$] on the inanga (*Galaxias maculatus*), albeit with a non-ratiometric CoroNa Green $Na^+$-sensitive dye (Lee *et al*., 2016).

## References


1. Abbas, L., Hajihashemi, S., Stead, L. A., Cooper, G. J., Ware, T. L., Munsey, T. S. Whitfield, T. T., White, S. J. (2011). Functional and developmental expression of a zebrafish Kir1.1 (ROMK) potassium channel homologue Kcnj1. *J. Physiol*. **589**(6), 1489-503.
2. Avella, M., Masoni, A., Bornancin, M., Mayer-Gostan, N. (1987). Gill morphology and sodium influx in the rainbow trout (*Salmo gairdneri*) acclimated to artificial freshwater environments. *J. Exp. Zool*. **241**(2), 159-69.
3. Bayaa, M., Vulesevic, B., Esbaugh, A., Braun, M., Ekker, M. E., Grosell, M., Perry, S. F. (2009). The involvement of SLC26 anion transporters in chloride uptake in zebrafish (D*anio rerio*) larvae. *J. Exp. Biol*. **212**, 3283-95.
4. Boisen, A. M., Amstrup, J., Novak, I., Grosell, M. (2003). Sodium and chloride transport in soft water and hard water acclimated zebrafish (Danio rerio). *Biochem. Biophys. Acta*. **1618**(2), 207-18.
5. Boron, W. F., de Weer, P. (1976). Intracellular pH transients in squid giant axons caused by $CO_2$, $NH_3$, and metabolic inhibitors. *J. Gen. Physiol*. **67**(1), 91-112.
6. Boyarsky, G., Hanssen, C. and Clyne, L. A. (1996). Superiority of in vitro over in vivo calibrations of BCECF in vascular smooth muscle cells. *FASEB J.* **10,** 1205-12.
7. Braun, M. H., Perry, S. F. (2001). Ammonia and urea excretion in the Pacific hagfish *Eptatretus stoutii*: Evidence for the involvement of Rh and UT proteins. *Comp. Biochem. Physiol*. **157**, 405-15.
8. Braun, M. H., Steele, S. L., Perry, S. F. (2009). The responses of zebrafish (Danio rerio) to high external ammonia and urea transporter inhibition: nitrogen excretion and

expression of rhesus glycoproteins and urea transporter proteins. *J. Exp. Biol*. **212**(23), 3846-56.

9. Buckler, K. J., Vaughan-Jones, R. D. (1990). Application of a new pH-sensitive fluoroprobe (carboxy-SNARF-1) for intracellular pH measurement in small, isolated cells. *Pflügers Arch*. **417**, 234-9.
10. Carter, N. W., Rector, F. C. Jr., Campion, D. S., Seldin, D. W. (1967). Measurement of intracellular pH of skeletal muscle with pH-sensitive glass microelectrodes. *J. Clin. Invest*. **46**, 920-33.
11. Chang, W. J., Horng, J. L., Yan, J. J., Hsiao, C. D., Hwang, P. P. (2009). The transcription factor, glial cell missing 2, is involved in differentiation and functional regulation of $H^+$-ATPase rich cells in zebrafish (*Danio rerio*). *Am. J. Physiol. Regul. Integr. Comp. Physiol*. **296**(4), R1192-201.
12. Chang, W. J., Wang, Y. F., Hu, H. J., Wang, J. H., Lee, T. H., Hwang, P. P. (2013). Compensatory regulation of $Na^+$ absorption by $Na^+/H^+$ exchanger and $Na^+$-$Cl^-$ cotransporter in zebrafish (*Danio rerio*). *Front. Zool*. **10**, 46.
13. Chen, Y., Mills, J. D., Periasamy, A. (2003). Protein localization in living cells and tissues using FRET and FLIM. *Differentiation*. **71**(9-10), 528-41.
14. Cruz, S. A., Chao, P. L., Hwang, P. P. (2013). Cortisol promotes differentiation of epidermal ionocytes through Foxi3 transcription factors in zebrafish (Danio rerio). *Comp. Biochem. Physiol. A. Mol. Integr. Physiol*. **164**(1), 249-57.
15. Dharmamba, M., Bornancin, M., Maetz, J. (1975). Environmental salinity and sodium and chloride exchanges across the gill of *Tilapia mossambica*. *J. Physiol. (Paris).* **70**(5), 627-35.

16. Dymowska, A. K., Hwang, P. P., Goss, G. G. (2012). Structure and function of ionocytes in the freshwater fish gill. *Respir. Physiol. Neurobiol*. **184**(3), 282-92.

17. Dymowska, A. K., Boyle, D., Schultz, A. G., Goss, G. G. (2015). The role of acid-sensing ion channels in epithelial Na+ uptake in adult zebrafish (Danio rerio). *J. Exp. Biol*. **218**, 1244-51.

18. Edsall, J. T., Carbon dioxide, carbonic acid, and bicarbonate ion: Physical properties and kinetics of interconversion. In: *$CO_2$, Chemical, biochemical and physiological aspects*. (Washington, D. C., 1970), pp 15-27.

19. Esaki, M., Hojishima, K., Kobayashi, S., Fukuda, H., Kawakami, K., Hirose, S. (2007). Visualization of zebrafish larvae of $Na^+$ uptake in mitochondrion-rich cells whose differentiation is dependent on *foxi3a*. *Am. J. Physiol. Regul. Integr. Comp. Physiol*. **292**(1), R470-80.

20. Esaki, M., Hoshijima, K., Nakamura, N., Munakata, K., Tanaka, M., Ookata, K., Asakawa, K., Kawakami, K., Wang, W., Weinberg, E. S., Hirose, S. (2009). Mechanism of development of ionocytes rich in vacuolar-type $H^+$-ATPase in the skin of zebrafish larvae. *Dev. Biol*. **329**(1), 116-29.

21. Eto, Y., Kobayashi, S., Nakamura, N., Miyagi, H., Esaki, M., Hojishima, K., Hirose, S. (2013). Close association of carbonic anhydrase (CA2a and CA15a), $Na^+/H^+$ exchanger (NHE3b), and ammonia transporter Rhcg1 in zebrafish ionocytes responsible for $Na^+$ uptake. *Front. Physiol*. **4**, 59.

22. Evans, D. H., Kormanik, G. A., Krasny, E., Jr. (1979). Mechanisms of ammonia and acid extrusion by the little skate *Raja erinacea*. *J. Exp. Zool*. **208**(3), 431-7.

23. Evans, D. H. (1980). Kinetic studies of ion transport by fish gill epithelium. *Am. J. Physiol*. **238**(3), R224-30.

24. Foskett, J. K., Scheffey, C. (1982). The chloride cell: definitive identification as the salt-secretory cell in teleosts. *Science*. **215**(4529), 164-6.

25. Furimsky, M., Moon, T. W., Perry, S. F. (1999). Intracellular pH regulation in hepatocytes isolated from three teleost species. *J. Exp. Zool*. **284**(4), 361-7.

26. Gillies, R. J. ,Ugurbil, K., den Hollander, J. A., Shulman, R. G. (1981). 31P NMR studies of intracellular pH and phosphate metabolism during cell division cycle of Saccharomyces cerevisiae. *Proc. Natl. Acad. Sci. USA*. **78**, 2125-9.

27. Girard, J. P., Payan, P. (1977). Kinetic analysis of sodium and chloride influxes across the gills of trout in fresh water. *J. Physiol*. **273**, 195-209.

28. Girard, J. P., Payan, P. (1980). Ion exchanges through respiratory and chloride cells in freshwater- and seawater-adapted teleosteans. *Am. J. Physiol*. **238**(3), R260-8.

29. Graber, M. L., DiLillo, D. C., Friedman, B. L., Pastoriza-Munoz, E. (1986). Characteristics of fluoroprobes for measuring intracellular pH. *Anal. Biochem*. **156**(1), 202-12.

30. Gruswitz, F., Chaudhary, S., Ho, J. D., Schlessinger, A., Pezeshki, B., Ho, C. M., Sali, A., Westhoff, C. M., Stroud, R. M. (2010). Function of human Rh based on structure of Rhcg at 2.1Å. *Proc. Natl. Acad. Sci. USA*. **107**(21), 9638-43.

31. Grynkiewicz, G., Poenie, M., Tsien, R. Y. (1985). A new generation of $Ca^{2+}$ indicators with greatly improved fluorescence properties. *J. Bio. Chem*. **260**(6), 3440-50.

32. Guh, Y. J., Lin, C. H., Hwang, P. P. (2015). Osmoregulation in zebrafish: ion transport mechanisms and functional regulation. *EXCLI J*. **14**:627-59.

33. Guh, Y. J., Tseng, Y. C., Yang, C. Y., Hwang, P. P. (2014). Endothelin-1 regulates $H^+$-ATPase-dependent transepithelial $H^+$ secretion in zebrafish. *Endocrinology*. **155**(5), 1728-37.

34. Harootunian, A. T., Kao, J. P. Y., Eckert, B. K., Tsien, R. Y. (1989). Fluorescence ratio imaging of cytosolic free $Na^+$ in individual fibroblasts and lymphocytes. *J. Biol. Chem*. **264**(32), 19458-67.

35. Heim, R., Tsien, R. Y., (1996). Engineering green fluorescence protein for improved brightness, longer wavelengths and fluorescence resonance energy transfer. *Curr. Biol*. **6**(2), 178-82.

36. Higashijima, S., Okamoto, H., Ueno, N., Hotta, Y., Eguchi, G. (1997). High-frequency generation of transgenic zebrafish which reliably express GFP in whole muscles or the whole body by using promoters of zebrafish origin. *Dev. Biol*. **192**(2), 289-99.

37. Hootman, S. R., Philpott, C. W. (1979). Ultracytochemical localization of Na+, K+-activated ATPase in chloride cells from the gills of a euryhaline teleost. *Anat. Rec*. **193**(1), 99-129.

38. Horng, J. L., Lin, L. Y., Huang, C. J., Katoh, F., Kaneko, T., Hwang, P. P. (2007). Knockdown of V-ATPase subunit A (atp6v1a) impairs acid secretion and ion balance in zebrafish (*Danio rerio*). *Am. J. Physiol. Regul. Integr. Comp. Physiol*. **292**(5), R2068-76.

39. Hossler, F. E., Musil, G., Karnaky, K. J. Jr., Epstein, F. H. (1985). Surface ultrastructure of the gill arch of the killifish, Fundulus heteroclitus, from seawater and freshwater, with special reference to the morphology of apical crypts of chloride cells. *J. Morphol*. **185**(3), 377-86.

40. Hwang, P. P., Lee, T. H., Lin, L. Y. (2011). Ion regulation in fish gills: recent progress in the cellular and molecular mechanisms. *Am. J. Regul. Integr. Comp. Physiol*. **301**(1), R28-47.

41. Hwang, P. P., Chou, M. Y. (2013). Zebrafish as an animal model to study ion homeostasis. *Pflügers Arch*. **465**, 1233-47.

42. Ito, Y., Kobayashi, S., Nakamura, N., Miyagi, H., Esaki, M., Hoshijima, K., Hirose, S. (2013). Close association of carbonic anhydrase (CA2a and CA15a), $Na^+/H^+$ exchanger (NHE3b) and ammonia transporter Rhcg1 in zebrafish ionocytesresponsible for $Na^+$ uptake. *Front. Physiol*. **4**, 59.

43. Iwai, T. (1969). On the "chloride cells" in the skin of larval puffer, *Fugu niphobles* (Jordan and Snyder). *La. Mer*. **7**(2), 26-31.

44. Jacobs, M. H., Stewart, D. R. (1942). The role of carbonic anhydrase in certain ionic exchanges involving the erythrocyte. *J. Gen. Physiol*. **25**(4), 539-52.

45. James-Kracke, M. R. (1992). Quick and accurate method to convert BCECF fluorescence to pHi: calibration in three different types of cell preparations. *J. Cell. Physiol.* **151,** 596-603.

46. Jezek, P., Mahdi, F., Garlid, K. D. (1990). Reconstitution of the beef heart and rat liver mitochondrial $K^+/H^+$ ($Na^+/H^+$) antiporter. Quantitation of $K^+$ transport with the novel fluorescent probe, PBFI. *J. Biol. Chem*. **265**(18), 10522-6.

47. Karnaky, K. J., Kinter, L. B., Kinter, W. B., Stirling, C. E. (1976). Teleost chloride cell II. Autoradiographic localization of gill Na,K-ATPase in killifish *Fundulus heteroclitus* adapted to low and high salinity environments. *J. Cell. Biol*. **70**, 157-77.

48. Kenworthy, A. K. (2001). Imaging protein-protein interactions using fluorescence resonance energy transfer microscopy. *Methods*. **24**(3), 289-96.

49. Kerstetter, T. H., Kirschner, L. B., Rafuse, D. D. (1970). On the mechanisms of sodium ion transport by the irrigated gills of rainbow trout (*Salmo gairdneri*). *J. Gen. Physiol*. **56**(3), 342-59.

50. Kim, J., Kim, Y. H., Cha, J. H., Tisher, C. C., Madsen, K. M. (1999). Intercalated cell subtypes in connecting tubule and cortical collecting duct of rat and mouse. *J. Am. Soc. Nephrol*. **10**, 1-12.

51. Krogh, A. (1938). Osmotic regulation in fresh water fishes by active absorption of chloride ions. *Z. Vgl. Physiol*. **24**(5), 656-66.

52. Kumai, Y., Perry, S. F. (2011). Ammonia excretion via Rhcg1 facilitates $Na^+$ uptake in larval zebrafish, Danio rerio, in acidic water. *Am. J. Physiol. Regul. Integr. Comp. Physiol*. **301**(5), R1517-28.

53. Kumai, Y., Nesan, D., Vijayan, M. M., Perry, S. F. (2012). Cortisol regulates Na+ uptake in zebrafish, Danio rerio, larvae via the glucocorticoid receptor. *Mol. Cell Endocrinol*. **364**, 113-25.

54. Kumai, Y., Kwong, R. W., Perry, S. F. (2014). The role of cAMP-mediated intracellular signalling in regulating Na+ uptake in zebrafish larvae. *Am. J. Physiol. Regul. Integr. Comp. Physiol*. **306**(1), R51-60.

55. Kwong, R. W. M., Kumai, Y., Perry, S. F. (2013). The role of aquaporin and tight junction proteins in the regulation of water movement in larval zebrafish (*Danio rerio*). *PLoS One*. **8**(8), e70764.

56. Kwong, R. W. and Perry, S. F. (2015). An essential role for parathyroid hormone in gill formation and differentiation of ion-transporting cells in developing zebrafish. *Endocrinology.* **156,** 2384-94.

57. Lee, J. A., Collings, D. A., Glover, C. N. (2016). A model system using confocal fluorescence microscopy for examining real-time intracellular sodium ion regulation. *Anal. Biochem*. **507**, 40-6.

58. Lee, Y. C., Yan, J. J., Cruz, S. A., Horng, J. L., Hwang, P. P. (2011). Anion exchanger 1b, but not sodium-bicarbonate cotransporter 1b, plays a role in transport functions in zebrafish H+-ATPase rich cells. *Am. J. Physiol. Cell Physiol*. **300**(2), C295-307.

59. Liao, B. K., Deng, A. N., Chen, S. C., Chou, M. Y., Hwang, P. P. (2007). Expression and water calcium dependence of calcium transporter isoforms in zebrafish gill mitochondrion-rich cells. *BMC Genomics*. **8**, 354

60. Lin, C. H., Shih, T. H., Liu, S. T., Hsu, H. H., Hwang, P. P. (2015). Cortisol regulates acid secretion of $H^+$-ATPase rich ionocytes in zebrafish (*Danio rerio*) embryos. *Front. Physiol*. **6**, 328

61. Lin, H., Randall, D. J. (1991). Evidence for the presence of an electrogenic proton pump on the trout gill epithelium. *J. Exp. Biol*. **161**, 119-134.

62. Lin, H., Randall, D. J. (1993). $H^+$-ATPse activity in crude homogenates of fish gill tissue: inhibitor sensitivity and environmental and hormonal regulation. *J. Exp. Biol*. **180**, 163-74.

63. Lin, T. Y., Liao, B. K., Horng, J. L., Yan, J. J., Hsiao, C. D., Hwang, P. P. (2008). Carbonic anhydrase 2-like a and 15a are involved in acid-base regulation and $Na^+$ uptake in zebrafish by $H^+$-ATPase rich cells. *Am. J. Physiol. Cell Physiol*. **294**(5), C1250-60.

64. Maetz, J., Garcia Romeu, F. (1964). The mechanism of sodium and chloride uptake by the gills of a freshwater fish – *Carassius aureus*. *J. Gen. Physiol*. **47**(6), 1195-207.

65. Maetz, J. (1973). $Na^+/NH_4^+$, $Na^+/H^+$ exchanges and $NH_3$ movement across the gills of *Carssius aureus*. *J. Exp. Biol*. **58**, 255-75.

66. Malgaroli, A., Milani, D., Meldolesi, J., Pozzan, T. (1987). Fura-2 measurement of cytosolic free $Ca^{2+}$ in monolayers and suspensions of various types of animal cells. *J. Cell. Biol*. **105**(5), 2145-55.

67. Malnic, G. (1988). Role of the kidney in controlling acid-base balance. *Child Nephrol. Uro*l. **9**, 241-52.

68. Marshall, W. S., Nishioka, R. S. (1980). Relation of mitochondria-rich chloride cells to active chloride transport in the skin of a marine teleost. *J. Exp. Zool*. **214**, 147-56.

69. McGinty, J., Taylor, H. B., Chen, L., Bugeon, L., Lamb, J. R., Dallman, M. J. and French, P. M. (2011). In vivo fluorescence lifetime optical projection tomography. *Biomedical optics express* **2,** 1340-50.

70. Mölich, A., Heisler, N. (2005). Determination of pH by microfluorometry: intracellular and interstitial pH regulation in developing early-stage fish embryos (*Danio rerio*). *J. Exp. Biol*. **208**, 4137-49.

71. Miller, S., Pollack, J., Bradshaw, J., Kumai, Y. and Perry, S. F. (2014). Cardiac responses to hypercapnia in larval zebrafish (Danio rerio): the links between CO2 chemoreception, catecholamines and carbonic anhydrase. *J. Exp. Biol.* **217,** 3569-78.

72. Miyawaki, A., Llopis, J., Heim, R., McCaffery, J. M., Adams, J. A., Ikura, M., Tsien, R. Y. (1997). Fluorescent indicators for $Ca^{2+}$ based on green fluorescent proteins and calmodulin. *Nature*. **388**(6645), 882-7.

73. Montrose, M. H. and Murer, H. (1986). Regulation of intracellular pH in LLC-PK1 cells by Na /H exchange. *J. Membr. Biol.* **93,** 33-42.

74. Murer, H., Hopfer, U., Kinne, R. (1976). Sodium/proton antiport in brush-border-membrane vesicles isolated from rat small intestine and kidney. *Biochem. J*. **154**, 597-604.

75. Nakada, T., Hoshijima, K., Esaki, M., Nagayoshi, S., Kawakami, K., Hirose, S. (2007). Localization of ammonia transporter Rhcg1 in mitochondrion-rich cells of yolk sac, gill, and kidney of zebrafish and its ionic strength-dependent expression. *Am. J. Physiol. Regul. Integr. Comp. Physiol.* **293**(4), R1743-53.

76. Nakhoul, N. L., Hering-Smith, K. S., Abdulnour-Nakhoul, S. M., Hamm, L. L. (2001). Transport of NH(3)/NH in oocytes expressing aquaporin-1. *Am. J. Physiol. Renal. Physiol*. **281**(2), F255-63.

77. Nasevicius, A., Ekker, S. C. (2000). Effective targeted gene "knockdown" in zebrafish. *Nat. Genet*. **26**(2), 216-20.

78. Nawata, C. M., Hung, C. C. Y., Tusi, T. K. N., Wilson, J. M., Wright, P. A., Wood, C. M. (2007). Ammonia excretion in rainbow trout (*Oncorhynchus mykiss*): evidence for Rh glycoprotein and $H^+$-ATPase involvement. *Physiol. Genomics*. **31**(3), 463-74.

79. Parks, S. K., Tresguerres, M., Goss, G. G. (2007). Interactions between Na+ channels and Na+-HCO3- cotransporters in the freshwater fish gill MR cell: a model for transepithelial Na+ uptake. *Am. J. Physiol. Cell Physiol*. **292**(2), C935-44.

80. Parks, S. K., Tresguerres, M., Goss, G. G. (2008). Theoretical considerations underlying $Na^+$ uptake mechanisms in freshwater fishes. *Comp. Biochem. Physiol*. **148**(4), 411-8.

81. Parks, S. K., Tresguerres, M., Galvez, F., Goss, G. G. (2010). Intracellular pH regulation in isolated trout gill mitochondrion-rich (MR) cell subtypes: evidence for Na+/H+ activity. *Comp. Biochem. Physiol. A. Mol. Integr. Physiol*. **155**(2), 139-45.

82. Payan, P., Matty, A. J., Maetz, J. (1975). A study of the sodium pump in the perfused head preparation of the trout *Salmo gairdneri* in freshwater. *J. Comp. Physiol*. **104**(2), 33-48.

83. Peek, W. D., Youson, J. H. (1979). Ultrastructure of chloride cells in young adults of the anadromous sea lamprey, Petromyzon marinus L., in fresh water and during adaptation to sea water. *J. Morphol*. **160**(2), 143-64.

84. Pelster, B., pH regulation and swimbladder function in fish. *Respir. Physiol. Neurobiol*. **144**, 179-90.

85. Perry, S. F., Wood, C. M. (1985). Kinetics of branchial calcium uptake in the rainbow trout: effects of acclimation to various external calcium levels. *J. Exp. Biol*. **116**, 411-33.

86. Pisam, M., Caroff, A., Rambourg, A. (1987). Two types of chloride cells in the gill epithelium of a freshwater-adapted euryhaline fish: Lebistes reticulatus; their modifications during adaptation to saltwater. *Am. J. Anat*. **179**(1), 40-50.

87. Pisam, M., Prunet, P., Boeuf, G., Rambourg, A. (1988). Ultrastructural features of chloride cells in the gill epithelium of Atlantic salmon, Salmo salar, and their modifications during smoltification. *Am. J. Anat*. **183**(3), 235-44.

88. Philpott, C. W. (1968). Halide localization in the teleost chloride cell and its identification by selected area electron diffraction. *Protoplasma*. **60**(1), 7-23.

89. Roberts, R. J., Bell, M., Young, H. (1973). Studies on the skin of plaice (*Pleuronectes platessa* L.). II. The development of larval plaice skin. *J. Fish Biol*. **5**, 103-8.

90. Roos, A., Boron, W. F. (1981). Intracellular pH. *Physiol. Rev*. **61**, 296-434.

91. Rothe, K. F. (1984). Changes in the extracellular pH value and its effect on the intracellular pH value of tissues. *Fortschr. Med*. **102**, 158-63.

92. Scheffey, C., Foskett, J. K., Machen, T. E. (1983). Localization of ionic pathways in the teleost opercular membrane by extracellular recording with a vibrating probe. *J. Membr. Biol*. **75**(3), 193-203.

93. Sekar, R. B., Periasamy, A. (2003). Fluorescence resonance energy transfer (FRET) microscopy imaging of live cell protein localizations. *J. Cell. Biol*. **160**(5), 629-33.

94. Shen, A. C. Y., Leatherland, J. F. (1978). Structure of the yolksac epithelium and gills in the early development stages of rainbow trout (*Salmo gairdneri*) maintained in different ambient salinities. *Envir. Biol. Fish*. **3**, 345-54.

95. Shih, T. H., Horng, J. L., Liu, S. T., Hwang, P. P., Lin, L. Y. (2012). Rhcg1 and NHE3b are involved in ammonium-dependent sodium uptake by zebrafish larvae acclimated to low sodium water. *Am. J. Phyisol. Regul. Integr. Comp. Physiol*. **302**(1), R84-93.

96. Sung, Y. H., Kim, J. M., Kim, H. T., Lee, J., Jeon, J., Jin, Y., Choi, J. H., Ban, Y. H., Ha, S. J., Kim, C. H., Lee, H. W., Kim, J. S. (2014). Highly efficient gene knockout in mice and zebrafish with RNA-guided endonucleases. *Genome Res*. **24**(1), 125-31.

97. Tang, C. H., Lee, T. H. (2007). The novel correlation between carbonic anhydrase II and anion exchanger 1 in gills of the spotted green pufferfish, Tetraodon nigrovirids. *J. Exp. Zool. A. Ecol. Genet. Physiol*. **307**(7), 411-8.

98. Thomas, R. C. (1977). The role of bicarbonate, chloride and sodium ions in the regulation of intracellular pH in snail neurons. *J. Physiol*. **273**, 317-38.

99. Truong, K., Sawano, A., Mizuno, H., Hama, H., Tong, K. I., Mal, T. K., Miyawaki, A., Ikura, M. (2001). FRET-based in vivo $Ca^{2+}$ imaging by a new calmodulin-GFP fusion module. *Nat. Struct. Biol*. **8**(12), 1069-73.

100. Ura, K., Soyano, K., Omoto, N, Adachi, S., Yamauchi, K. (1996). Localization of Na+, K(+) ATPase in tissues of rabbit and teleosts using an antiserum directed against a partial sequence of the alpha-subunit. *Zoolog. Sci*. **13**(2), 219-27.

101. Urasa, F. M., Wendelaar Bonga, S. E. (1987). Effects of calcium and phosphate on the corpusles of Stannius of the teleost fish, *Oreochromis mossambicus*. *Cell Tissue Res*. **249**(3), 681-90.

102. Varsamos, S., Nebel, C. and Charmantier, G. (2005). Ontogeny of osmoregulation in postembryonic fish: a review. *Comp. Biochem. Physiol. A. Mol. Integr. Physiol.* **141,** 401-29.

103. Vaughan-Jones, R. D. (1979). Regulation of chloride in quiescent sheep-heart Purkinje fibres studied using intracellular chloride and pH-sensitive micro-electrodes. *J. Physiol*. **295**, 111-37.

104. Walsh, P. J. (1986). Ionic requirements for intracellular pH regulation in rainbow trout hepatocytes. *Am. J. Physiol*. **250**, R24-9.

105. Wagner, C. A., Kovacikova, J., Stehberger, P. A., Winter, C., Benabbas, C., Mohebbi, N. (2006). Renal acid-base transport: old and new players. *Nephron Physiol*. **103**, 1-6.

106. Wang, Y. F., Tseng, W. C., Yan, J. J., Hiroi, J., Hawng, P. P. (2009). Role of SLC12A10.2, a Na-Cl cotransporter-like protein, in a Cl uptake mechanism in zebrafish (Danio rerio). *Am. J. Physiol. Regul. Integr. Comp. Physiol*. **296**(5), R1650-60.

107. Westerfield, M. (1994). *The Zebrafish Book: A Guide for the Laboratory Use of Zebrafish (Danio rerio).* (University of Oregon, Institute of Neuroscience, Eugene, OR)

108. Wright, P. A., Wood, C. M. (1985). An analysis of branchial ammonia excretion in the freshwater rainbow trout: effects of environmental pH change and sodium uptake blockade. *J. Exp. Biol*. **114**, 329-53.

109. Wright, P. A., Wood, C. M. (2009). A new paradigm for ammonia excretion in aquatic animals: role of Rhesus (Rh) glycoproteins. *J. Exp. Biol*. **212**, 2303-12.low-$Na^+$ and acidic environments. *Am. J. Physiol. Cell Physiol*. **293**(6), C1814-23.

110. Yan, J. J., Chow, M. Y., Kaneko, T., Hwang, P. P. (2007). Gene expression of $Na^+/H^+$ exchanger in zebrafish $H^+$-ATPase rich cells during acclimation to low-$Na^+$ and acidic environments. *Am. J. Physiol. Cell Physiol*. **293**(6), C1814-23.

111. Yucha, C. (2004). Renal regulation of acid-base balance. *Nephrol. Nurs. J*. **31**, 201-6.